AD-481 994

PILOT-INDUCED OSCILLATIONS: THEIR CAUSE AND ANALYSIS

I. L. Ashkenas, et al

June 1964

SYSTEMS TECHNOLOGY, INC. STI

Norair Report NCR-64-143

Systems Technology, Inc., Report STI TR-239-2

PILOT-INDUCED OSCILLATIONS: THEIR CAUSE AND ANALYSIS

Irving L. Ashkenas
Henry R. Jex
Duane T. McRuer

20 June 1964

Performed under

Norair Division, Northrop Corporation

Letter Agreement 8914-62-382
24 July 1964
and Amendments

DISCLAIMER NOTICE

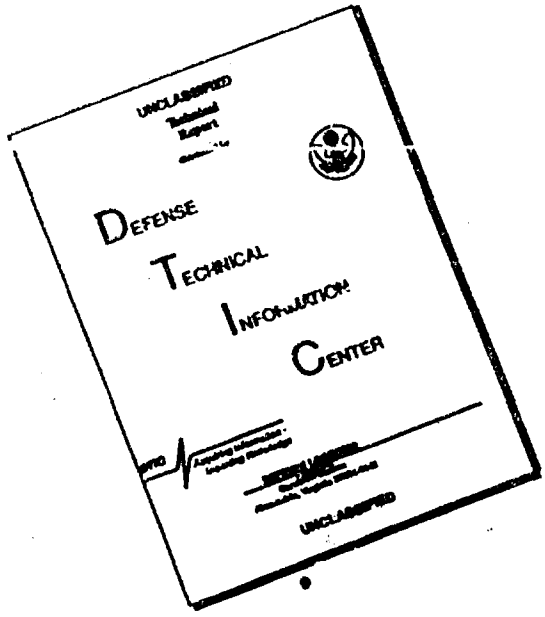

THIS DOCUMENT IS BEST QUALITY AVAILABLE. THE COPY FURNISHED TO DTIC CONTAINED A SIGNIFICANT NUMBER OF PAGES WHICH DO NOT REPRODUCE LEGIBLY.

The National Technical Information Services distributes declassified (unclassified and unlimited) reports to the general public in accordance with a Memorandum of Understanding between NTIS and the Defense Supply Agency, Department of Defense.

Declassified (unclassified and unlimited) reports are those technical documents which have been determined by competent authority under the provisions of Executive Order No. 11652, March 8, 1972, and current Department of Defense Directives, as no longer required to be kept secret in the interests of the National defense or foreign policy.

This report has been declassified and cleared for public release under the above provisions, and no security restrictions are imposed upon its use and disclosure.

ABSTRACT

Systems analysis techniques are applied to the problem of pilot-induced aircraft oscillations (PIO). Mathematical models used for the pilot prior to and during PIO, as well as the use of various pilot and subsystem describing functions, are reviewed. Several examples of PIO causes, analyses, and cures are given, including linear and nonlinear longitudinal PIO. The closed-loop describing function for a rate-limited position servo is derived in the Appendix.

FOREWORD

This report summarizes several years of intermittent work conducted at Systems Technology, Inc., on the problem of pilot-induced oscillations. The major portions of the efforts reported were performed either as part of other handling qualities studies under Contract new AF 33(616)-5661 for the Flight Control Laboratory of the Air Force Systems Command, or as part of an investigation of T-38A and general PIO problems for Northrop-Norair under ~~Letter Agreement~~ 8914-62-382 dated 24 July 1962, and subsequent amendments. This report itself has been almost totally drafted under the Norair agreement.

The major contributors to these efforts, and to this report, are listed as authors. Other STI engineers who have also contributed in some way or other to STI's PIO studies include: D. Graham, W. A. Johnson, V. J. Kovacevich, C. P. Shortwell, J. Wolkovitch, and C. D. Wezeman. The authors are most grateful to both Mr. D. L. Hirsch of the Vehicle Dynamics and Control Branch, Norair, and Mr. R. J. Wasicko, who served as the AF Project Engineer—their guidance, constructive comments, support, and patience have played an extremely important role in these studies.

CONTENTS

FIGURES

TABLES

SECTION I

INTRODUCTION

A pilot-induced oscillation (PIO) is an inadvertent sustained oscillation of the pilot–vehicle system. Throughout aviation's history PIO's of various degrees of severity have appeared sporadically. Indeed, the static instability of the Wright Flyer resulted in a mild longitudinal oscillation of that most early pilot–vehicle system. With very high performance aircraft having fully powered control systems, PIO's have become more frequent; and also more lethal, because relatively small pilot forces can cause a rapid buildup to catastrophic loads. Many of these cases appear, embarrassingly, during final flight tests or early production stages; thus there are few well-documented cases on public record. Some exceptions are reported in Refs. 1–4, 18, and 19. Two of these references (1 and 4) present a rare, and unusually complete, time history of a PIO. This dramatic recording, which has great value in providing physical appreciation for the phenomena involved in PIO's, is reproduced in Fig. 1. The PIO occurred in an early version of the T-38 aircraft (since modified to completely eliminate the possibility of recurrence) following the shut-off of an oscillating pitch damper in a mistrimmed position. Besides providing a beautiful example of events in a PIO buildup sequence which will be elaborated further below, this record with its ±8g oscillations offers graphic experimental evidence of a situation which pilots will not willingly duplicate.

The often violent and unexpected nature of many forms of PIO's has usually lead to a prompt attempt to "cure" the condition (quietly). Although there is no generally valid theory for predicting PIO's, two lines of approach (Ref. 2) can be indicated:

1. Compare the open-loop dynamic characteristics of the aircraft plus manual controls with those dynamic characteristics of other craft which, as shown by experience, are compatible with the presence or absence of PIO's.

FIGURE 1

TIME HISTORY OF A P.I.O.

T-38A # AF 58-1104 (N-5103)
FLIGHT 8, RUN 7, JAN 26, 1960
WT = 11,690 lb, CG = 16% MAC
M = 0.91 h = 6500 ft V_t = 540 Kts

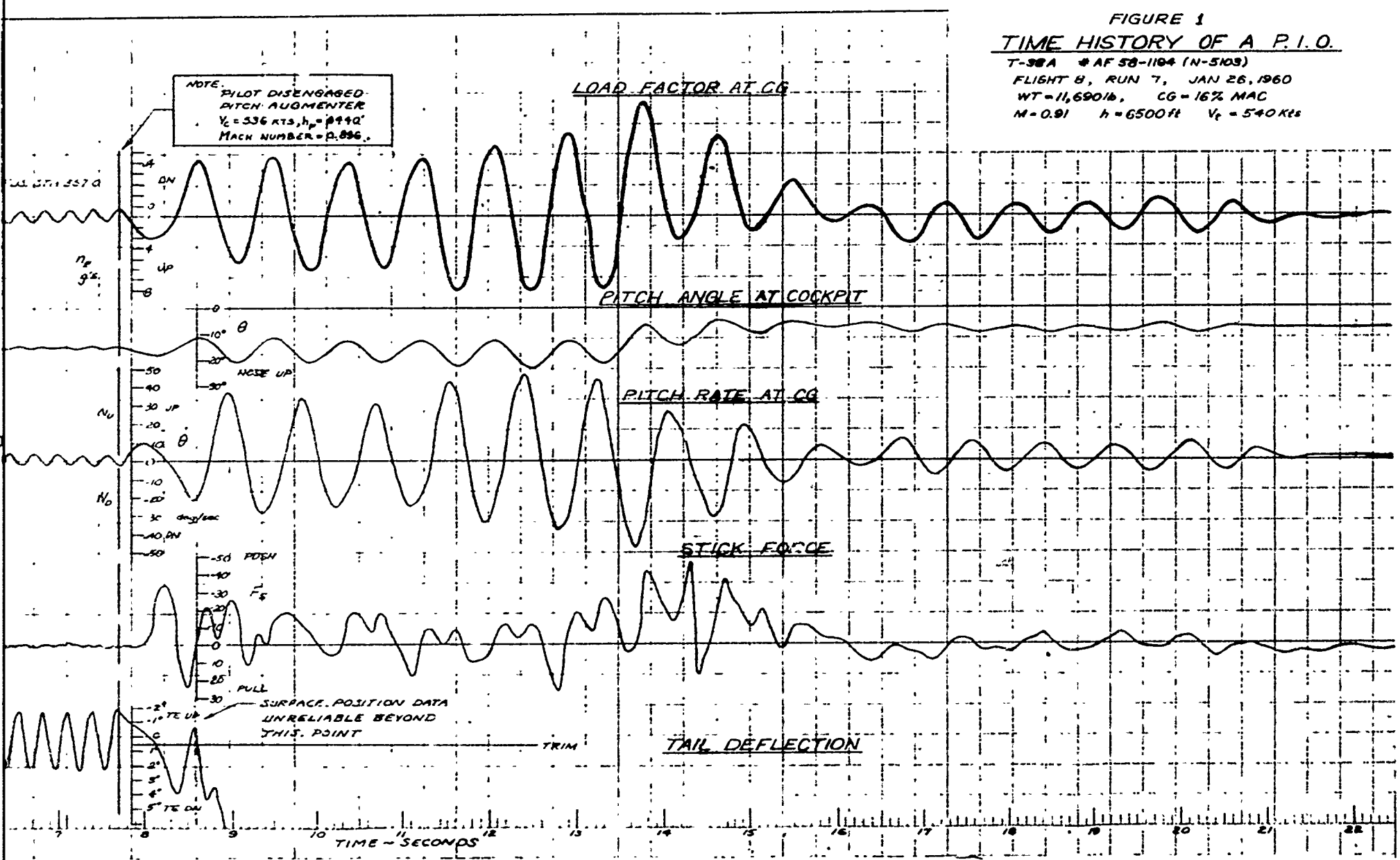

2. Perform closed-loop stability analyses of the pilot–vehicle system using appropriate describing function representations for the pilot, vehicle, and manual control system.

At one limit the first approach leads to a catalog of vehicle-plus-control-system sinusoidal-input describing functions which represent either PIO-prone or PIO-resistant configurations. By their nature such data are extremely valuable as points of departure, although they are usually too specific to be directly useful on other vehicle configurations. An attempt to generalize on PIO–resistant characteristics for a linear vehicle is given in Ref. 2. Referring to the airframe's frequency response for dynamic stick force per g, it is noted that: [When the steady-state stick force per g is itself satisfactory] "...experience shows that unsatisfactory dynamic characteristics of the pilot–airframe combination and pilot-induced oscillations are avoided when the amplitudes of the control-force-gradient frequency response are never less than the low-frequency asymptote." In practice this corresponds to a short-period damping ratio of $1/\sqrt{2}$ or higher. More recent experience (e.g., Refs. 5 and 6) indicates that such a high damping ratio is not essential to avoid PIO's, so the quoted statement represents a sufficient rather than necessary condition. However, some such specification is desirable for its simplicity, and, perhaps, as still more experience is gained, a similar statement can ultimately be refined to include both necessary and sufficient conditions.

In the meantime one can either overspecify on the basis of applicable experience (the first-listed approach) or treat PIO problems using a servoanalytic attack (the second-listed approach). The latter approach has been used for some time with considerable success to provide physical explanations of PIO occurrences and to enhance appreciation of the effects of fixes on PIO tendencies (e.g., Refs. 1–4, 7 and 20). The techniques used provide a measure of prediction as well as understanding. The approach is limited by incomplete knowledge of the range and applicability of possible human-pilot describing functions. However, the state of such knowledge has progressed through the years, especially with respect to closed-loop handling qualities theory, so some statements can now be made with greater certainty than previously. One purpose of this report is to bring the

state of the art of PIO technology up to date via the systems analysis approach which has been successful in the related field of handling qualities research (Refs. 9–12).

The over-all system to be analyzed in PIO problems encompasses complex dynamic interactions between the pilot, artificial feel devices, powered control surfaces, airframe, and display subsystems. To this general complexity are added the following complications:

Adaptive behavior by the pilot

The presence of unavoidable or intentional nonlinearities (such as friction, dead zones, and preload) in the control system

Often neglected aerodynamic terms (such as the elevator's contribution to the normal acceleration felt by a pilot and, for lateral PIO, the aileron's adverse yaw)

In turn, describing the adaptive pilot requires a valid mathematical model, the nonlinearities require consideration of the specific task and disturbance inputs, and the aerodynamic subtleties require a thorough understanding of the airframe transfer functions. In spite of the total complexity of the pilot–vehicle system containing these elements, PIO's can and have been successfully analyzed and predicted by careful system analyses of the types to be described herein.

The report starts with a brief resume of the systems approach to the analysis of the pilot–vehicle system in Section II. This lays the foundation for Section III, which introduces and categorizes the basic causes of PIO. Section IV contains selected examples of the system analysis of PIO situations, and covers both the diagnostic and the curative aspects of the problem encountered. Mathematical derivation of a describing function needed in Section IV, but not available elsewhere, is contained in the Appendix.

SECTION II

THE PILOT-VEHICLE SYSTEM

A. GENERAL DESCRIPTION

Among the significant attributes of a human pilot are his ability to establish a wide variety of pilot-vehicle system organizations (i.e., many different system structures or effective block diagrams) and adjustments therein. This repertory of behavior is so extensive that the pilot, as an adaptive controller, has capabilities which exceed those of the most sophisticated unmanned control system. From a systems analysis standpoint this variety may at first seem discouraging. For many flight control situations, however, further consideration indicates that all is not hopeless. In controlling any complex system, successful behavior is very narrowly limited. The very nature of the requirements for "good" control system performance and the restrictions imposed by the dynamic characteristics of the controlled element constrain the successful human pilot to operate in accord with well-established "laws." When well trained and motivated, or when the imposed restrictions are severe, the performance of the pilot and the system can be predicted with an accuracy sufficient for many engineering purposes. The prediction is both qualitative and quantitative. In short, the man-machine system can be made amenable to mathematical analysis (Refs. 13 and 16).

Experiment has shown that the system organizations and adjustments adopted by the pilot for single-loop or uncoupled multiloop feedback systems are consistent with those of "good" feedback systems in general. This presumes, of course, that the adjustments which are required do not violate the capabilities of the human operator. Thus, the system will be organized and adjusted as if done by a "super-servoanalyst." In the case of more complicated multiloop systems, direct experimental data on pilot adjustment and organization do not yet exist. However, comparison of experimental results with analytical inferences obtained with an extended

pilot model strongly suggests that the pilot model and analysis methods have a continuing practical validity. In fact, as the number of possible display and control alternatives increases, the most fruitful criteria yet found for choosing the dominant loop closures are simply those which the "super-servoanalyst" would choose.

B. INPUT-OUTPUT MODELS

The models used in pilot-vehicle systems analyses are input-output operators, that is, transfer functions and describing functions. In the case of constant-coefficient linear systems the **transfer function** is simply given by the Cramer's Rule solution of the equations of motion when written in Laplace transform form. Thus transfer functions are ratios of rational polynomials in the Laplace operator, s; the denominator is the characteristic equation of the system, while the numerator connects a specific output with specific forcing terms. Substitution of $j\omega$ for s in the transfer function will yield the "frequency response." The frequency response relates, via an input/output amplitude ratio and phase angle difference, the fundamental-sinusoid component of the system output to the sinusoidal input. (If the system is stable the total output will approach the sinusoidal component of the output as time goes by and the transients die away).

The extension of the basic notion of an input-output operator to describe the input-output characteristics of nonlinear elements is fraught with subtle mathematical difficulties (Ref. 15) but can easily be visualized. Physically, in most oscillatory circumstances the input to the nonlinearity is usually close to a sinusoid, whereas the output of the nonlinearity is periodic but may depart considerably from a sinusoidal shape. This distorted waveform reflects the presence of higher harmonic components induced by the nonlinearity. In their transmission about the loop, these harmonics are substantially suppressed in amplitude by the lags of the airframe and control system. Because they largely disappear in transit, the input to the nonlinearity is scarcely affected by these higher harmonics, and thus retains its nearly sinusoidal nature. So, insofar as stability considerations are concerned, the inputs and outputs of most of the nonlinear

elements of interest in PIO (nonlinear gearing, friction, breakout, etc.) can be approximated by a pair of sine waves of suitable amplitude and phase shift.

The appropriate sinusoidal approximations for both the input and the output of the nonlinearity are the fundamental components of the Fourier series representation of the actual waveforms. Then, analogous to transfer functions, the "sinusoidal-input describing function" is defined as the amplitude ratio and phase shift between the fundamental components of the input and output. However, the output waveform from a nonlinear element at any given input frequency may vary as the input amplitude varies, so each nonlinearity requires a family of describing functions at specified input levels. In fact, it is the often adverse changes with input amplitude (in the describing function amplitude ratio and phase shift) which lead to sustained closed-loop system oscillations. The use of rational polynomials to represent sinusoidal describing functions for nonlinear systems is only justified in the frequency domain; and the substitution therein of the Laplace operator, s, for $j\omega$ is not meaningful. Thus, it is not strictly correct to plot a conventional root locus diagram for a loop closed around a nonlinearity, though in many cases this is done to help describe qualitatively the effect of the nonlinearity. The only strictly valid portion of such nonlinear root loci is on the $j\omega$ axis, and on the particular locus family corresponding to a certain input amplitude at the nonlinear element. It also follows that the transient response of nonlinear systems cannot be calculated from information in the sinusoidal describing function.

C. PILOT MODELS

Two phases or types of manual control system behavior must be considered in a PIO analysis. These are:

1. Prior to a PIO the pilot is exerting on-the-average control of more-or-less random inputs and has adopted a quasi-stationary set of feedbacks (displayed or sensed quantities) and equalizations (gains, lead, lag) which are compatible with "good" control (i.e.,

small error, stability, low effort, etc.). Several control loops may be present, although only one or two are usually dominant.

2. After a PIO is developed, the apparent airframe motions change from a random-like to a nearly sinusoidal form.

Corresponding to these two types of system behavior are two quite different varieties of pilot and nonlinear element describing functions. For the first phase, at least some basic portions of the total control system, as organized by the pilot, are compensatory (the total control system may have pursuit elements inserted by the pilot, see Ref. 14, but these will not affect those system aspects relating to stability), and the appropriate models are Gaussian-input describing functions. For inanimate elements these are known only for the simplest of nonlinearities, but for the pilot the Gaussian-input describing function for compensatory situations is fairly well established. Figure 2 contains a brief summary and Ref. 16 a simple, more complete treatment of the state of this knowledge.

The probable pilot behavior for any given vehicle flight condition and task prior to the PIO can be estimated using the model of Fig. 2 directly, although some simplifications are usually made (see Refs. 9-16, and especially Refs. 13 and 16). The essence of the simplified adaptation rules is that the pilot adopts a form of equalization such that the pilot-plus-vehicle open-loop describing function is much greater than 1.0 at low frequencies while approximating a -20 db/decade slope in the region of crossover frequency, ω_c. These adjustments satisfy the conflicting demands of good closed-loop control at the input frequencies lower than ω_c (below ω_c, $|Y_{OL}| \gg 1$; thus $|Y_{CL}| \doteq 1.0$), and adequate stability (at ω_c an adequate phase margin exists). Recent experiments by Systems Technology, Inc., and The Franklin Institute (Ref. 25) show that under laboratory conditions, the crossover frequencies for a given controlled element are constant so long as $\omega_c > \omega_i$ (where ω_i is the effective bandwidth of the system forcing function). This constancy of ω_c does not extend across different controlled elements, but ranges from 3 to 8 rad/sec, the lower for control of pure inertias and the higher for control of pure gain elements. Comparison of

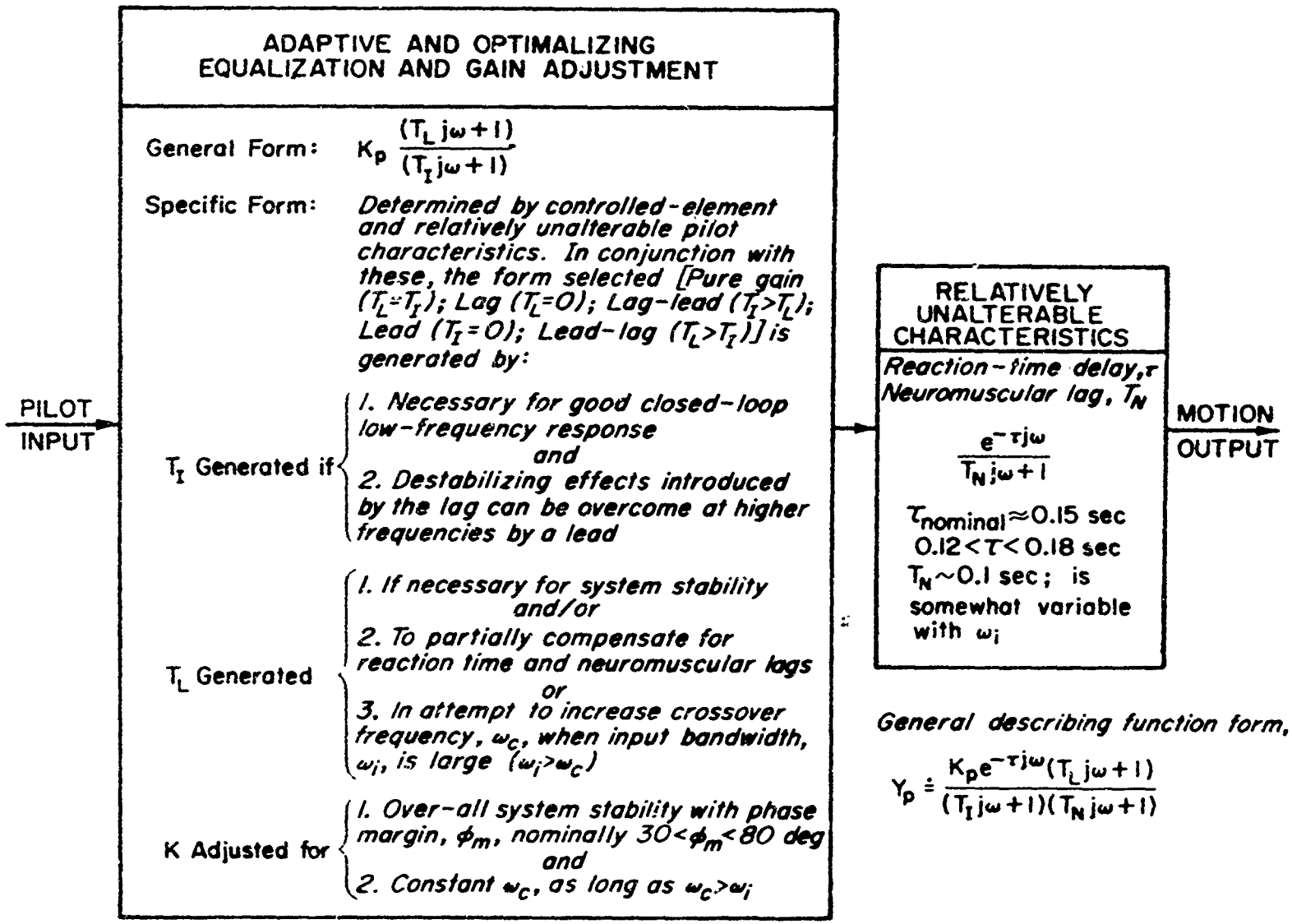

Figure 2. Generalized Human Pilot Describing Function Model for a Compensatory System with Random-Appearing Visual Inputs

ω_c measured in flight versus simulator shows that about half the laboratory value of ω_c is realized (Ref. 38). In general, the simplified rule of thumb for pre-PIO adaptation is: **Make $|Y_{OL}| = |Y_p \cdot Y_c| \doteq |\omega_c/s|$ in the vicinity of $\omega_c \doteq 1.0$ to 2.0 rad/sec.**

For the second, or actual PIO phase, the dominant loops must be treated with sinusoidal-input describing function models. The state of knowledge for this periodic-input case is almost the opposite of that for random inputs. Here a great deal is known about sinusoidal-input describing functions for inanimate nonlinear elements, but some critical information is lacking on sinusoidal-input models for the pilot. The present hypothetical pilot describing function model for PIO derives from sinusoidal-input frequency response measurements in manual control systems (Refs. 26-31). In these studies, conducted with a pure gain controlled element, a key observation is that the terminal phase of pilot adaptation is "synchronous," or "precognitive" behavior. In other words, once the pilot recognizes that his input is a sinusoid, he essentially duplicates the sinusoid with no phase lag—basically $Y_p \doteq K_p$. This nondelayed behavior breaks down above 3 cps or so.

PIC investigations using a $Y_p \doteq K_p$, with visual inputs (e.g., pitch angle) presumed, have had a distinct measure of success (e.g., Ref. 1, 7, and 20) in determining probable causes and assessing cures for existing PIO's. Despite these successes the confidence level in the $Y_p \doteq K_p$ form for the human pilot sinusoidal-input describing function is not too high. For instance, in most PIO's the pilot has adapted to the pre-PIO situation with lead or lag or lag-lead equalization generated as the occasion demands. The question then arises as to whether the pilot retains the equalization as the PIO begins, or whether he abandons the equalization and attempts synchronous behavior with essentially zero phase lag. The effective reaction time delay no longer exists in his response. Also, for a pure gain controlled element the usual low frequency lag equalization present for random inputs is dropped for the sinusoidal-input case. But it is not clear whether a net phase angle, made up of the sum of the leads and lags in the previous equalization, is dropped or retained in the PIO for

controlled elements other than $Y_c = K_c$. This question is important in determining the gain reduction required to re-establish stable control and in estimating whether or not a PIO is likely to occur for a specific flight situation. New experimental research is needed on this matter.

Between the pre-PIO and developed-PIO phases is a transient period which contains the excitation, vehicle change, pilot-organized system change, etc., which serves to initiate the PIO. This transient takes a finite time, during which all stationary descriptions of pilot behavior are invalid. The only method which can be used at this state of the art is to analyze the closed-loop dynamics both before and during a PIO to see if conditions conducive to sustained oscillations exist.

D. PILOT INPUTS AND OUTPUTS FOR PIO

The easiest way to represent the pilot inputs and outputs is on a block diagram. A typical block diagram of a pilot-vehicle system is shown in Fig. 3 for longitudinal PIO, and similar block diagrams can be drawn for other axes. Representative mathematical models for various system elements for a fighter-type aircraft are shown at the bottom of Fig. 3.

The inputs to the pilot prior to a PIO consist of those visual and motion cues which are used to perform the basic flying task at hand. Most of the complex piloting tasks involve aircraft attitude relative to a real or artificial horizon as the inner loop. In other cases, such as climb programming or LABS maneuvers, the normal acceleration indicator may be in dominant use. Another task in which PIO is frequently encountered is formation flying, where the cues are a complex combination of linear displacements, attitudes, and angular rates.

Once a PIO limit cycle has been established, the input situation is not so well understood experimentally. However, one of the dominant inputs is certainly the physical acceleration felt by the pilot, and others are the gross motions of the outside-world horizon. Experience has shown that most of the PIO situations and pilot behavior can be

FIGURE 3. SIGNIFICANT CONTROL LOOPS FOR PILOT–AIRFRAME COUPLING DURING PITCH CONTROL

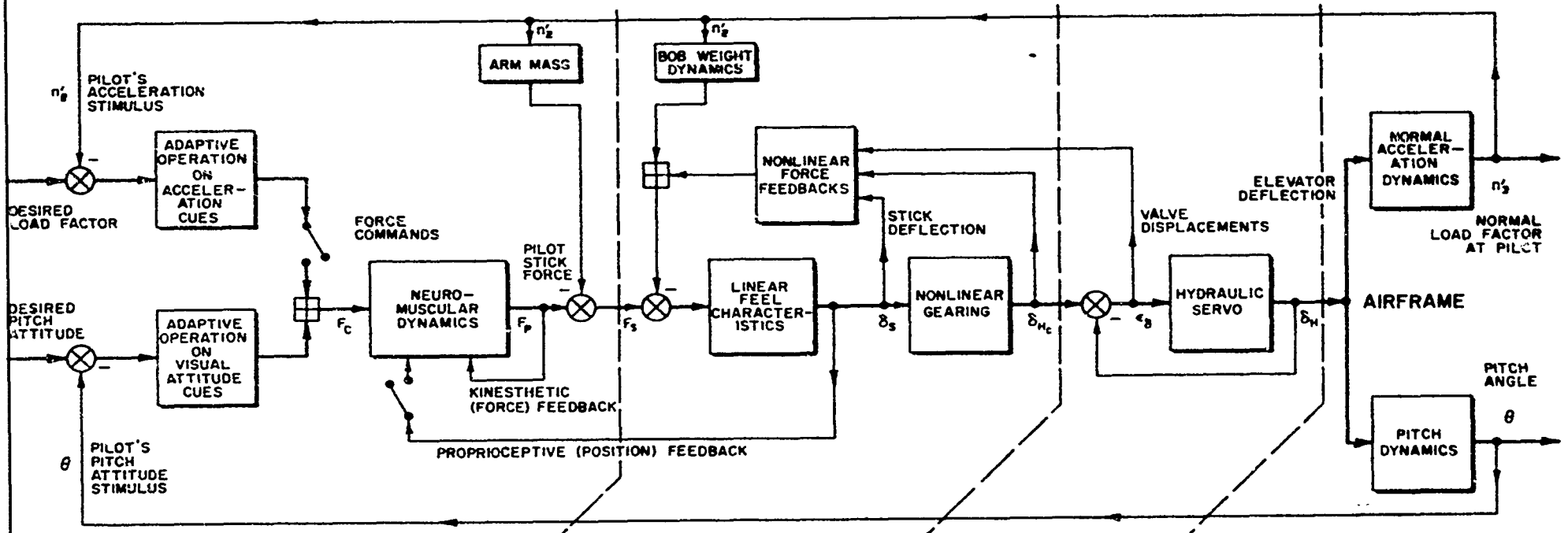

INTERNAL TO PILOT — FEEL SYSTEM — SERVO — AIRFRAME

$$Y_p(s) = \frac{F_s \text{ or } \delta_s}{\theta \text{ or } n'_z} = \frac{K_p e^{-\tau s}(T_L s + 1)}{(T_N s + 1)(T_I s + 1)}$$

Reaction Time: $\tau \doteq .2$ sec
Neuromuscular Lag: $T_N = 0 \rightarrow .1$ sec
Rate Sensitivity: $T_L = 0 \rightarrow 1.0$ sec
Integral Sensitivity: $T_I \doteq 0 \rightarrow 10$ sec
Pilot Force Gain: $K_{p_\theta} \doteq 50 - 500$ lb/rad

Linear Characteristics:

$$\frac{\delta_{H_c}}{F_s} = K_\delta \frac{1}{\frac{s^2}{\omega_F^2} + \frac{2\zeta_F}{\omega_F} s + 1}$$

$K_\delta = .0035$ rad/lb, $\omega_F \doteq 18$, $\zeta_F \doteq .18$

Nonlinear Characteristics:
- Stick Preload
- Stick Friction
- Hysteresis in Linkage
- Nonlinear Gearing
- Nonlinear Bobweight

Linear:

$$\frac{\delta_H}{\delta_{H_c}} \doteq \frac{1}{T_S s + 1}$$

$T_S \doteq .02 \rightarrow .07$ sec

Nonlinear:
- Rate Saturation

Linear: (Including quasi steady aero and inertial elastic effects

$$\frac{\theta}{\delta_H} = \frac{K_\theta (T_{\theta_2} s + 1)}{s\left(\frac{s^2}{\omega_{sp}^2} + \frac{2\zeta_{sp}}{\omega_{sp}} s + 1\right)}$$

$$\frac{n'_z}{\delta_H} = \frac{K_{n'_z}\left(\frac{s^2}{\omega_h^2} + \frac{2\zeta_h}{\omega_h} s + 1\right)}{\left(\frac{s^2}{\omega_h^2} + \frac{2\zeta}{\omega_{sp}} s + 1\right)}$$

$K_\theta \doteq 5$ rad/rad
$T_{\theta_2} \doteq .3$ sec
$\omega_{sp} \doteq 7$ rad/sec
$\zeta_{sp} \doteq .4$
$K_{n'_z} \doteq 145$ g/rad
$\omega_h \doteq 24$ rad/sec
$\zeta_h \doteq .15$

Nonlinear:
- Nonlinear M(α)

understood by considering the attitude and/or normal accelerations as the dominant sensed quantities.

The pilot outputs of interest are the forces and displacements applied to his "manipulator," i.e., control stick or pedals. As Fig. 3 shows, a pilot has both force and displacement control loops within his neuromuscular actuator system. A great deal of (largely intuitive) controversy has raged over whether the pilot output should be considered to be essentially a force or essentially a displacement. In the more sophisticated context of Fig. 3, this resolves to the question of the relative degrees of "tightness" of the force and displacement loops. An answer, with its qualifying details, has not yet been obtained, although some experimental programs are under way to help establish the fundamental neuromuscular processes involved. The pertinent main points which have evolved from extensive experience to date are:

1. Both force (kinesthetic) and displacement (proprioceptive) feedbacks are used for control by the neuromuscular system.
2. With spring-restrained manipulators the displacement outputs seem to be dominant (high displacement loop gain) when large or preprogrammed manipulator motions are required, whereas the force outputs are dominant (low displacement loop gain) when fine motions and precision control are needed.
3. Even with tight closure of the displacement loop, such as occurs when a free-moving pure displacement manipulator, the high frequency dynamic characteristics of the neuromuscular system show more lag than those evident with a "stiff-stick" pressure control.

The second point above qualitatively agrees with experience on longitudinal and lateral controls. Thus the force-feel characteristics of the aircraft control system seem to be more critical than the displacement characteristics for small-motion longitudinal control. This implies that the pilot's neuromuscular system displacement loop is operating at low gains since, otherwise, a tight proprioceptive loop would suppress many of the control system's objectionable force nonlinearities. In

aileron control, on the other hand, control motions can be more gross and less emphasis on the minimization of force-type nonlinearities is needed.

Summarizing these results, it appears that either force or position outputs may be dominant in PIO studies, depending on the situation being considered and the nonlinearities present. One should, therefore, check the pilot-vehicle system characteristics for both force and displacement inputs from the pilot to see if conditions for a sustained limit cycle can be found. Further experiments related to these problems are planned.

SECTION III

BASIC CAUSES OF PIO

A. SEQUENCE OF EVENTS

Certain necessary steps in a sequence are common to most PIO's. Before discussing these from the standpoint of PIO causes, consider first some of their physical attributes. Figure 1 clearly illustrated the following sequence:

1. The pilot is initially adapted to some control situation between the extremes of precise tracking maneuvers and hands-off flight.
2. Something causes a sudden change in the situation dynamics. This could be a change in the pilot's organization of the system, the initiation of a large steady maneuver, a damper failure, etc. (In Fig. 1 the change followed the shutdown transient of a faulty pitch damper, which left the elevator in a mistrimmed position.)
3. An oscillation builds up and is sustained for a few cycles; a legitimate limit cycle exists. (Note that two sets of limit cycles exist in Fig. 1 for times greater and less than 15 sec.)
4. Finally, the pilot either lets go, freezes the stick, or puts in a well-timed maneuver to kill the oscillation.

The conditions that lead to step 3 that are the root "cause" of a PIO. It is always possible, by making the forward loop gain high enough, to drive any physical closed-loop system unstable. Pilot trainees or test pilots feeling out a new aircraft often tighten up on their control response enough to provide one or two oscillations indicating incipient instability. If this tendency is easy to avoid, and if a modest reduction in pilot gain (e.g., 25 to 50 percent) can remove the instability, then such situations do not usually end up as serious PIO cases. It is those unusual situations where several factors combine to make the pilot-vehicle

instability region either impossible to avoid or difficult to get out of that are the real concern of this report.

There are several instances where a sustained oscillation of the vehicle-plus-control-systems alone may be triggered by a large pilot-induced maneuver (e.g., bobweight plus nonlinear gearing). Although such oscillations do not involve visual or acceleration feedbacks through the pilot's higher centers, they often depend on the presence of the pilot's arm on the stick. Thus the pilot's neuromuscular system is involved, and the oscillations are still "caused" by the pilot. Such oscillations are often unavoidable because it is seldom practical to completely let go of the stick, especially at the high-subsonic, low-altitude conditions where the problem is aggravated.

B. PILOT-REFERENCED CAUSES OF PIO

There are several ways of looking at the causes of a PIO. One is to catalog all the PIO situations ever recorded, including all the necessary subsystem details, etc., and then to say that each combination of vehicle and subsystems when combined with the pilot was the cause of a PIO. Another way is to note that certain system phenomena, such as stick-force-to-control-deflection hysteresis, often lead to PIO when other conditions are right and can thus cause PIO. A third way, and one which seems to transcend the difficulties of the previous two, is to say that certain inherent human physical limitations are the basic cause for any PIO. This is not to degrade the human pilot's role but, instead, to emphasize it, because it is unlikely that any black-box could be devised which is as clever and effective in coping with unmanageable controlled elements as a skilled pilot. Were it not for the pilot's versatile gain adaptability, many flight conditions would be unstable. But there is a limit to the rapidity with which the human can adapt, and this can sometimes lead to a PIO.

When referred to the pilot, then, the basic causes of PIO seem to fall into the following categories:

1. Incomplete pilot equalization

   a. Incomplete training

   b. Inappropriate transfer of adaptation (i.e., carryover of improper techniques from another aircraft)

2. Excessive demands on pilot adaptation

   a. Required gain, lead, or lag lie outside the range of normal capabilities

   b. Rate of adaptation is too slow to preclude oscillation

   c. Inadequate capability to cope with system nonlinearities

3. Limb-manipulator coupling

   a. Impedance of neuromuscular system (including limb) on control stick or pedals changes feel system dynamics

   b. Motion-induced limb force feedback (e.g., arm becomes a bobweight)

Incomplete Pilot Equalization is a common problem and results from insufficient time or trials with the given situation for the pilot to achieve a good, stable closure. The cure, of course, is more training, and more than one PIO problem has disappeared as the piloting technique is refined. In some instances the required piloting technique may be quite different from that with which the pilot is familiar, and a difficult transition period results. If the analyses show that no equalization is needed by the pilot prior to a PIO, but that the required pilot gain is very low (i.e., control is very sensitive), then incomplete pilot gain adjustment may well cause PIO tendencies. Due to the temporary nature of these tendencies, this cause of PIO is not considered as serious as some of the others.

Excessive Demands on Pilot Adaptation are the most common cause of malignant PIO's. The ranges of lead, lag, and gain available to the pilot are fairly broad, but there are some limitations which can result in a sustained oscillation. Experience on fixed-base flight simulators

indicates that a pilot can change his gain over nearly two decades if given enough time (Ref. 13). However, for a sudden change in the required pilot gain, a 2:1 variation (±6 db) is easily accomplished, but a 4:1 change (±2 db) is apparently quite difficult, at least for aircraft control tasks. The achievable lead time constants measured in the STI-FIL experiments range from $T_L = 0$ to greater than 5 sec, while achievable lags range from $T_I = 0$ to 10 sec. The pilot can easily adopt small leads roughly equal to his reaction time delay, but the generation of small lags in the vicinity of 0.1 to 1 sec requires relatively longer training. As noted previously, when a transient oscillation starts to dominate the input, the pilot seems to revert to a pure gain behavior, thus dropping his previous equalization. In certain situations, where the pilot has adopted a lag equalization to compensate for a high-frequency, low-damped pure second-order controlled element, dropping the lag equalization can seriously destabilize the system, leading to a series of quasi-steady PIO's as the pilot is forced to backpedal severalfold on his gain to restabilize the system. This cause of PIO may be difficult to prove at the present state of the art.

By far the most excessive demands on pilot adaptation are caused by various nonlinearities in the control system. Certain forms of complex series nonlinearity, such as elevator-to-stick-force hysteresis or rate limiting inside a closed-loop system, defy the pilot's ability to compensate or invert it, and some degree of PIO becomes inevitable during tight closed-loop control. These problems can be readily treated and understood by analytical methods to be described later.

The last category of PIO causes is related to Limb-Manipulator Coupling. This is a general term for certain dynamic interactions such as the effect of the pilot's arm mass acting like a bobweight and thus feeding back local accelerations into the control system. This type of coupling can actually destabilize the short-period mode if the feel system natural frequency is nearby, and if the pilot does not fight the acceleration loads on his arm. A more subtle, but possible, PIO cause is the mass-like impedance of the pilot's arm (or legs) on the controls when he is loosely hanging on to the

stick. Depending on the apparent arm mass "seen" by the feel system, its natural frequency can be lowered enough that coupling forces (e.g., bobweight) can drive the short-period feel system combination unstable (Refs. 1 and 7). Both types of limb-manipulator effects need further investigation using moving-base simulators.

In the next section it is shown that, in classifying the types of physical phenomena and analysis techniques associated with PIO, there appears to be a natural division into linear and nonlinear categories. Correlating the examples given later in Table I with the basic causes just described, reveals that the "linear" types of PIO are usually caused by the first category (Incomplete Pilot Equalization), while the nonlinear types of PIO all fall into the second category (Excessive Demands on Pilot Adaptation). Although the correspondence should not be drawn too closely, it is not fortuitous and was one reason for the scheme chosen to categorize the types and causes of PIO.

SECTION IV

ANALYSIS OF PIO

A. GENERAL APPROACH

The object of PIO analysis is to determine the fundamental controlled element problems which could cause an oscillation when the pilot, represented by a describing function, attempts to close the control loop. The basic approach to the analysis of PIO is to select a potentially critical aircraft and flight condition; then to analyze this condition, using servoanalysis techniques and various pilot models representing reasonable piloting behaviors, to determine whether either zero damping (in a linear system) or a limit cycle (for a nonlinear system) can exist. When a diagnostic analysis is required, the critical flight conditions where PIO are suspected or experienced are usually given at the outset, although other flight conditions, with no record of PIO (or in regions where no PIO is expected) should also be examined to check the validity of the results. For a prognostic (at the design stage) analysis, election of potential PIO-prone flight and control system conditions is primarily a matter of identifying situations which contain one or more characteristics inimical to pilot-vehicle system stability. To some extent this can be made deductive, e.g., by cataloging conditions representing dynamic response extremes in the control system and vehicle; but experience and knowledge of past PIO history, with its indications of possible parallels, provide the best guide. This will be discussed further in the next subsection.

The analyst is cautioned to examine all possibilities for PIO before settling on the dominant cause, since experience has shown that more than one, and usually a combination of, PIO-enhancing factors are involved in any particular problem.

In subsections to follow PIO's are classified, and the corresponding critical systems and conditions are discussed. Next, some typical steps

and data required in any PIO analysis are reviewed. This material will help to define the scope of test and analytical work required. Finally, four examples of distinctly different PIO problems will be presented to illustrate the range of problems, the techniques, and the forms of mathematical models which are involved in PIO analyses.

B. CLASSIFICATION OF PIO

The profusion of individual cases of PIO which have been and will be encountered requires some unifying classification scheme. Of the several alternatives possible, the following scheme seems to be the best suited from the point of view of the physical phenomena involved and the type of analysis required:

> PIO's are <u>classed</u> by the control axis involved, i.e., as longitudinal (pitch), lateral (roll), directional (yaw), and coupled lateral-directional.
>
> The <u>type</u> is defined by the nature of the physical phenomena (and, incidentally, the kind of analysis) involved:
>
> I. Oscillations due to linear pilot-vehicle coupling
>
> II. Limit cycles due to one or more nonlinear elements in <u>series</u> in the primary control loop
>
> III. Limit cycles due to one or more nonlinear elements in vehicle motion <u>feedback</u> paths subsidiary to the primary control loop
>
> The <u>species</u> of PIO within each class and type describe the specific character of each individual case of PIO.

From an analysis standpoint, the <u>class</u> distinction directly indicates the appropriate equations of vehicle motion. The <u>type</u> definition orders the problem in terms of analytical rather than physical complexity. Thus Type I systems require only linear analysis methods, although the systems may be multiloop in nature, whereas Type II and Type III systems always require nonlinear analysis techniques. Type II systems are essentially single-loop insofar as the nonlinear analysis is concerned, but Type III systems are always multiloop. The <u>species</u> description is intended to

emphasize physical rather than analytical characteristics, so it may provide only anecdotal information.

As an example of the classification scheme, the "J. C. Maneuver" would be categorized as an oscillation in the pitch axis (class) involving nonlinearities in the feel system (type), and characterized by a-rapid-oscillation-at-large-load-factors-during-flight-maneuvers-at-high-dynamic-pressure (species). Several known or suspected PIO cases are classified using the above bases in Table I. As a partial substitute for direct experience, Table I can be of significant help with either diagnostic or prognostic PIO analyses. In the former case, when the nature of the PIO can be identified with one of those shown, the available references and type of analysis required are immediately apparent. In the latter case, when predictions of potential PIO problems for a new design are required, Table I shows the most likely possibilities, as well as those amenable to simple analysis at the preliminary design stage. Also shown in Table I are the critical flight conditions and critical subsystems for each of the species of PIO listed. Each listing follows the order Species (Aircraft)$^{Ref.}$; Critical Subsystem; Critical Flight Condition; Remarks, and makes use of the shorthand legend identified at the bottom of the table.

C. DATA AND STEPS REQUIRED

Experience has shown that the detailed nature of the subsystem dynamics must be at hand for a meaningful analysis to be undertaken. For the simplest type of PIO (those involving linear pilot-vehicle coupling) only one more-or-less unique transfer function for each subsystem need be known. However, many PIO involve subsystem nonlinearities of varying degrees of complexity. For such instances sinusoidal-input describing function techniques have proven to be most useful, and so it becomes essential to obtain the various subsystem describing functions for various levels of input to the nonlinear elements. Table II has been prepared as a guide to the scope of information required for each critical subsystem as indicated in Table I. The items in Table II are by no means exhaustive, and serve merely to indicate the scope of information required and the form in which it will prove most useful.

TABLE I

CLASSIFICATION OF SOME KNOWN PIO CASES

Examples shown as: SPECIES (Aircraft)[Ref.]; Critical Subsystem; Critical Flight Condition; Remarks

CLASS	TYPE
	I. LINEAR
PITCH	IMPROPER SIMULATION[5]; D, V; a: Abnormally high value of $1/T_{\theta_2}$ and low $\zeta_{\omega_{sp}}$ led to zero ζ_{sp} when regulating large disturbances. GCA-INDUCED PHUGOID (C-97)[39]; D, V; b: Lag from radar-detected error to voice command led to unstable closed-loop phugoid mode. ARM ON STICK (A4D-1)[7], (T-38A)[1]; F; a: Arm mass increases feel system inertia; leads via B feedback to unstable coupling with short-period dynamics if pilot merely hangs loosely onto stick after a large input.
LATERAL-DIRECTIONAL	ω_p/ω_ϕ EFFECT (X-15)[20], (T-33VSA)[21], (F-101B)[34], (F-106A), (KC-135A)[33], (B-58); V; c: Zeros of roll/aileron transfer function are higher than Dutch roll frequency, $\lvert\omega_p/\omega_\phi\rvert > 1.0$, leading to closed-loop instability at low ζ_d conditions. BORESIGHT OSCILLATIONS (F-5A); D, V; c: Spiral roll mode driven unstable if roll information is degraded during gunnery.
YAW	FUEL SLOSH SNAKING (KC-135A)[33], (T-37A)[32]; V; c: Fuel slosh mode couples with Dutch roll mode when rudder used to stop yaw oscillation.
ROLL	NONE KNOWN

Legend:

Superscripts refer to references of occurrence.

Critical Subsystems:

D = Display
F = Feel system (except B)
B = Bobweight
S = Power servo actuator
V = Vehicle (airframe)
A = Augmenter (damper)

Critical Flight Conditions:

a = Low altitude, near-sonic Mach
b = Landing approach or takeoff
c = Cruise

TABLE I (Cont'd)

CLASS	TYPE
	II. SERIES NONLINEAR ELEMENTS
PITCH	PORPOISING (SB2C-1)[37]; F; c: Hysteresis in stick versus elevator deflection resulted in low frequency speed and climb oscillations. J. C. MANEUVER (F-86D), (F-100C); F, S; a: Valve friction plus compliant cabling resulted in large oscillations at short period. PITCH-UP (XF-104, (F-101B)[34], (F-102A)[36]; V; c: Unstable kink in M(α) curve led to moderate-period oscillations of varying amplitudes (depending on extent and nature of the kink) during maneuvers near the crtical angle of attack. LANDING PIO (X-15)[22]; S; b: Closed-loop around elevator rate-limiting caused moderate oscillations at short period.
LATERAL-DIRECTIONAL	
YAW	TRANSONIC SNAKING (A3D); V, F; a, c: Separation over rudder causes control reversal for small deflections, leading to limit cycle if rudder used to damp yaw oscillations.
ROLL	PILOT-INDUCED CHATTER (F-104B)[35]; A; c: Small limit cycle due to damper aggravated whenever pilot attempted to control it.

CLASS	TYPE
	III. SUBSIDIARY FEEDBACK NONLINEAR ELEMENTS
PITCH	BOBWEIGHT BREAKOUT (A4D-1)[2,7], (T-38A)[1,4]; F, B; a: At high-g maneuvers the bobweight overcomes system friction and reduces apparent damping of the aircraft in response to force inputs, resulting in large oscillations at short period. LOSS OF PITCH DAMPER
LATERAL-DIRECTIONAL	LOSS OF YAW DAMPER
YAW	
ROLL	

TABLE II

SUBSYSTEM DATA REQUIRED FOR PIO ANALYSES

SUBSYSTEM	DATA REQUIRED
D = Displays	Type of presentation: Compensatory versus pursuit. Instrument dynamics: θ_D/θ, n'_{z_D}/n'_z, etc. Kinematics of visual field: e.g., horizon visibility, orientation in formation flight, visual landing aids.
F = Feel System (excl. B)	Control surface commands due to stick force and displacement: Frequency response, $\delta_c/F_s = f\|F_s\|$, $\delta_c/\delta_s = f\|\delta_s\|$; three levels of F_s or δ_s, for at least one decade centered at ω_{sp}. Static data on friction, hysteresis loop in δ_c versus F_s, etc. For nonlinear stick gearing, take describing function data near $\delta_{c_{trim}}$.
B = Bobweight	Bobweight force feedback dynamics: F_{s_B}/a'_z, $F_{s_B}/\ddot{\theta}$, etc. Bobweight breakout and hysteresis as $f(n'_z)$, etc. Equivalent bobweight location, considering all mass unbalance which is sensitive to n_z and $\ddot{\theta}$. Possibly include inertial bending and support deflection under n_z loads as B effects, if not already in vehicle dynamics.
S = Servo Actuator	Control output/input frequency response and describing function: δ/δ_c at three levels of δ_c; also $\delta_{e_{max}}$, $\dot{\delta}_{e_{max}}$, threshold, etc.
A = Augmenter (Damper)	Control commands due to vehicle motions: δ_{c_A}/body rates; describing functions if nonlinear; threshold, limits, etc.
V = Vehicle (Airframe)	Specific configuration and flight conditions: Compatible weights, inertias, α, q, δ_{trim}, $n_{z_{trim}}$, M_{trim}, etc. Calculate transfer functions or measure frequency response (for constant $\|\delta\|$): a_i/δ (a_i = accel. at c.g., pilot, effective B location, etc.); attitude/δ (attitude = θ or φ or ψ, etc., or corresponding rates). Preferably include inertial and aeroelastic bending here; also Z_{δ_e} or Y_{δ_r} effects.

The principal steps involved in any analysis of pilot-induced oscillations are as follows:

1. Select the dominant control mode (e.g., pitch attitude control), critical flight conditions, and dominant subsystems likely to be directly involved in any oscillation (see Tables I and II).
2. Obtain, either by analysis of measurement, the required transfer functions or describing functions of the critical systems as specified in Table II.
3. Assume an oscillating output at selected levels (either observed or estimated), then perform a closed-loop describing function analysis to verify if the conditions required to sustain the oscillation can be reasonably expected. Two or more levels of oscillation may be necessary to cover the extremes of the subsystem nonlinear describing functions. Use a pure gain model for the pilot.
4. Check to see whether the pilot gain required in the limit cycle is consistent with the probable magnitude of the pilot's Gaussian-input describing function adapted prior to the onset of PIO (magnitude of Y_p at the PIO frequency). The methods of Ref. 13 or 16 should be used to estimate the pre-PIO pilot adaptation for the specific control task involved.
5. If conditions for an oscillation are compatible with Steps 3 and 4, then a PIO is likely, provided the assumed mode of pilot control (e.g., attitude error to force output) is valid.
6. The analysis should be duplicated for any other likely pilot control modes or nonlinearity amplitudes, and the predicted PIO tendencies weighted according to the results therefrom.

D. EXAMPLE CASES

The examples to follow will illustrate potential PIO situations of increasing analytical complexity, corresponding to the type of classification given above. The first two cases involve no nonlinearities whatever, so both illustrate Type I situations. The third example considers a piloted-force nonlinearity which is analytically tractable; the nonlinear system element is also in series with the primary control and hence

the control situation is Type II. Finally, the fourth example treats a Type III system which is so complex that it can be feasibly analyzed only at the two extremes of nonlinear behavior.

1. Example 1: Linear Control of Short-Period Longitudinal Motions

Consider the pitch control of an aircraft at high subsonic speeds and low altitude. As noted earlier, in a sustained PIO the pilot's sinusoidal describing function can be considered a simple gain ($Y_p \doteq K_p$). Under such circumstances and assuming that his primary response is to visual pitch-attitude cues,* the pilot-vehicle open-loop describing function at any limit cycling frequency, ω, is given by

$$\frac{\theta}{\theta_\epsilon} = Y_p(s) \cdot \frac{\theta}{\delta_e}(s) = \frac{K_p M_{\delta_e}\left(s + \frac{1}{T_{\theta_2}}\right)}{s\left(s^2 + 2\zeta_{sp}\omega_{sp}s + \omega_{sp}^2\right)} \tag{1}$$

where $s = j\omega$ and phugoid motions are neglected. Accordingly, the closed-loop characteristic equation is given by

$$\begin{aligned}\Delta' &= s\left(s^2 + 2\zeta_{sp}\omega_{sp}s + \omega_{sp}^2\right) + K_p M_\delta\left(s + \frac{1}{T_{\theta_2}}\right) \\ &= s^3 + s^2\left(2\zeta_{sp}\omega_{sp}\right) + s\left(\omega_{sp}^2 + K_p M_\delta\right) + K_p M_\delta\left(\frac{1}{T_{\theta_2}}\right)\end{aligned} \tag{2}$$

The usual factored form of Δ' is expressed as follows, where the prime denotes closed-loop parameters:

---

*It should be emphasized here that in spite of accompanying vertical accelerations, attitude cues will be those the pilot consciously uses in attempting to get out of a PIO situation, so the above considerations are valid. Nevertheless, acceleration inputs introduced by the pilot's arm bobweight effect acting through control system friction could be a nonlinear destabilizing influence. The fourth example considers such effects in detail.

$$\Delta' = \left(s + \frac{1}{T_c}\right)\left(s^2 + 2\zeta'_{sp}\omega'_{sp}s + \omega'^2_{sp}\right)$$

$$= s^3 + s^2\left(\frac{1}{T_c} + 2\zeta'_{sp}\omega'_{sp}\right) + s\left(\omega'^2_{sp} + \frac{2\zeta'_p\omega'_{sp}}{T_c}\right) + \frac{\omega'^2_{sp}}{T_c} \qquad (3)$$

Since a sustained oscillation implies zero damping, the conditions for PIO (and the only condition for which Eq 3 has meaning, because of the assumed oscillation) correspond to those for which $\zeta'_{sp}\omega'_{sp}$ is zero. Equating the s^2 coefficients of Eq 2 and 3,

$$2\zeta'_{sp}\omega'_{sp} + \frac{1}{T_c} = 2\zeta_{sp}\omega_{sp}$$

and the condition for an oscillation becomes

$$2\zeta'_{sp}\omega'_{sp} = 2\zeta_{sp}\omega_{sp} - \frac{1}{T_c} = 0 \qquad (4)$$

Thus, if $1/T_c$ is forced to equal $2\zeta_{sp}\omega_{sp}$, by the use of sufficiently high gain, the system <u>can</u> be driven unstable. To better appreciate this possibility, consider the root locus plot given in Fig. 4. The relationship of Eq 4 is graphically illustrated here, and conclusions as to the maximum value of $1/T_c$ and minimum value of $2\zeta'_{sp}\omega'_{sp}$ are clearly shown to be

$$\left(\frac{1}{T_c}\right)_{max} \rightarrow \frac{1}{T_{\theta_2}}$$

$$\left(2\zeta'_{sp}\omega'_{sp}\right)_{min} \rightarrow 2\zeta_{sp}\omega_{sp} - \frac{1}{T_{\theta_2}} \qquad (5)$$

Probable values for the right side of Eq 5 can be obtained by considering the approximate airframe transfer function factors given in Ref. 17,

$$2\zeta_{sp}\omega_{sp} = -(Z_w + M_q + M_{\dot{\alpha}})$$

$$\frac{1}{T_{\theta_2}} \doteq -Z_w + \frac{Z_\delta}{M_\delta} M_w \qquad (6)$$

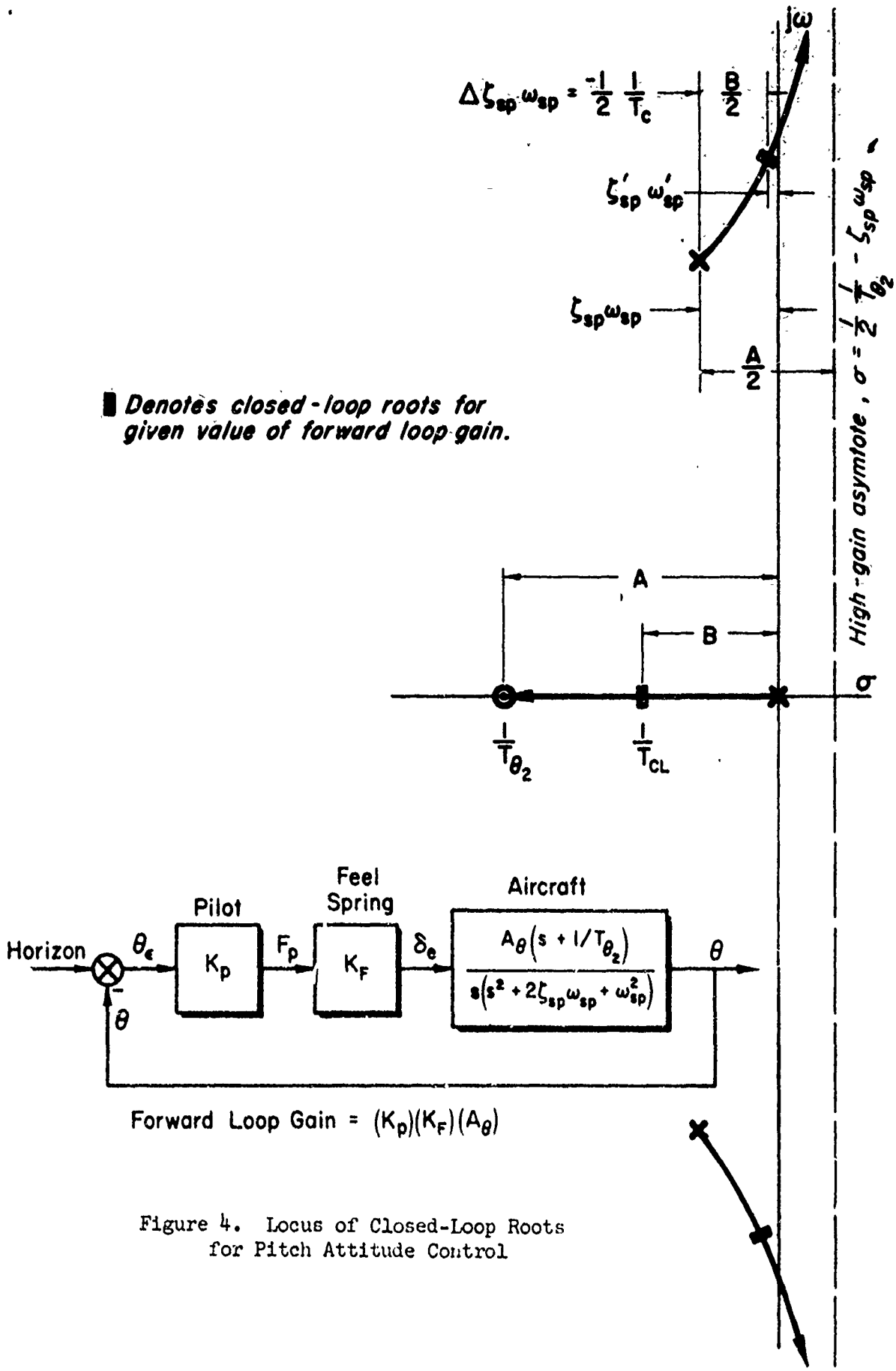

Figure 4. Locus of Closed-Loop Roots for Pitch Attitude Control

so that $$2\zeta_{sp}\omega_{sp} - \frac{1}{T_{\theta_2}} \doteq -M_q - M_{\dot{\alpha}} - \frac{Z_{\delta_e}}{M_{\delta_e}} M_w$$

$$\doteq \frac{\rho S U_o c^2}{4I_y}\left(-C_{M_q} - C_{M_{\dot{\alpha}}} + \frac{2k_y^2}{c l_\delta} C_{M_\delta}\right) \qquad (7)$$

where $l_\delta = cC_{M_\delta}/C_{L_\delta}$ is the effective elevator control arm (measured positive forward). For conventional tail-aft airplanes with some static margin (l_δ and $C_{M_{\dot{\alpha}}}$ both negative) the bracketed terms of Eq 7 are always positive. For a canard control, l_δ will change sign, and the $C_{M_{\dot{\alpha}}}$ contribution will be negative, so it is conceivable that the entire term could be negative. However, a general observation is that it will take a very unusual kind of configuration (small l_δ, low values of $-C_{M_q}$, which, for conventional airplanes, is usually an order of magnitude greater than $C_{M_{\dot{\alpha}}}$, etc.) to make the value of $2\zeta_{sp}\omega_{sp} - 1/T_{\theta_2}$ negative, as sketched in Fig. 4. Therefore only for such unusual airframe configurations is there a possibility of driving $\zeta'\omega'$ to zero to achieve a sustained PIO.

The foregoing demonstrates that for airplanes with negligible control system dynamics (including nonlinear elements or bobweight effects), longitudinal PIO's involving only attitude control are essentially impossible. However, in variable-stability flight testing and ground-based simulation studies where the general practice is to hold Z_w constant and vary ζ_{sp}, ω_{sp}, stick force and displacement per g, etc., artificial relationships between $\zeta_{sp}\omega_{sp}$ and $1/T_{\theta_2}$ can lead to PIO's of the simple type under consideration here. For example, the data of Ref. 5, reproduced in Fig. 5, show PIO "tendencies" for the lower left region of the ζ, ω plane. These data were obtained for a fixed value of Z_w corresponding to $1/T_{\theta_2} = 3.22$ for all the conditions tested. The theoretical boundary for zero ζ'_{sp} as given in Eq 5 is superposed on the original plot. It may be seen that there is general agreement between the predicted possible "simple" PIO region to the left of the boundary and the observed region. The fact that the experimental region for very light stick-force gradients lies somewhat to the right of the theoretical boundary is evidence of additional dynamics—in this case nonlinear effects due to the high ratio of breakout-force-to-stick-gradient, 1.2 lb/1.0 lb/g.

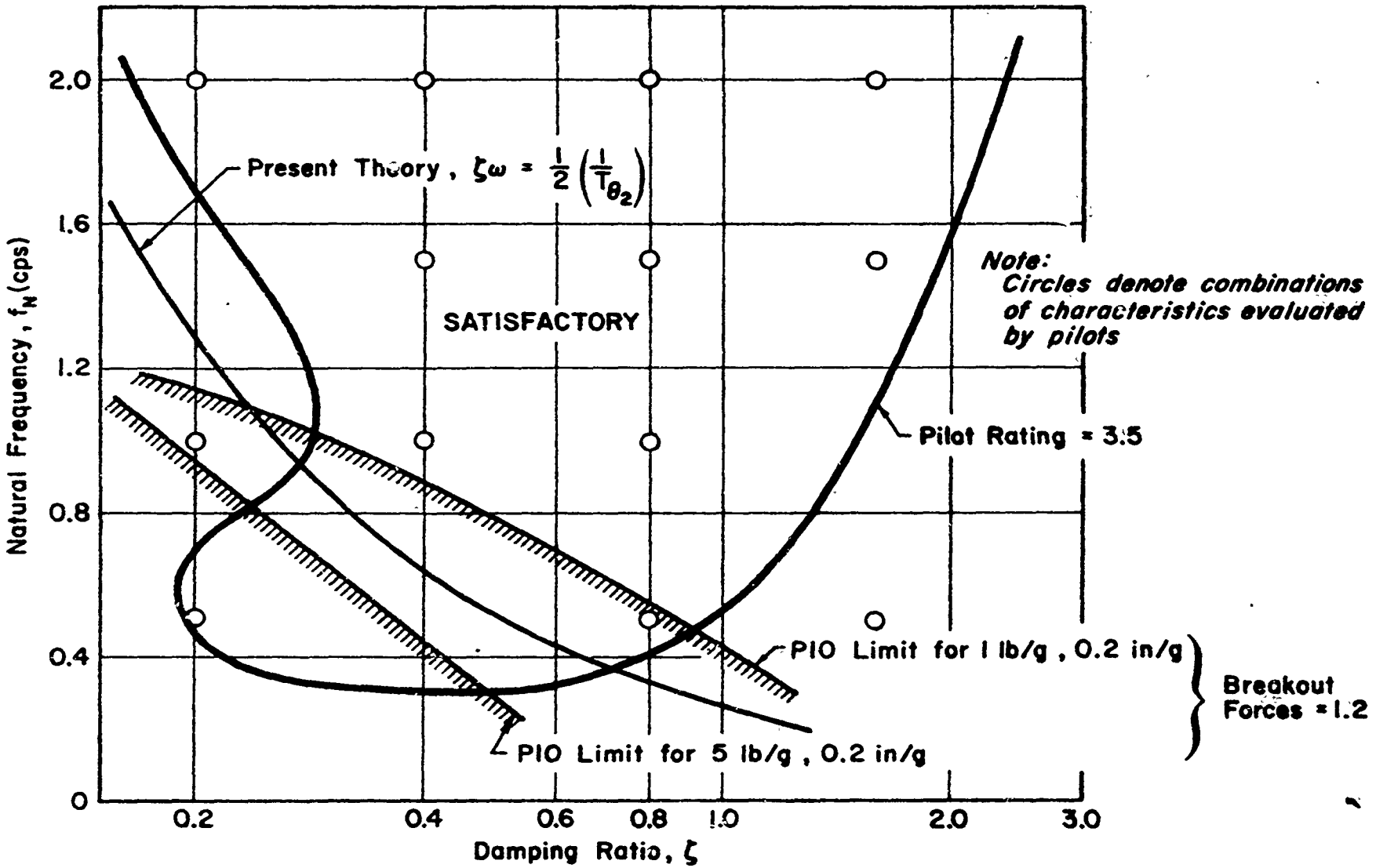

Figure 5. Pilot Acceptance and PIO Boundaries for Short-Period Stability Characteristics

Although the possibility of simple PIO's exists to the left of the boundary, whether they in fact will occur depends on the likely value of pilot-vehicle system gain. Thus a further analysis requires an examination of the probable pilot's "mid-frequency" gain for normal closed-loop control prior to the PIO, and comparison of this gain level with the mid-frequency gain required to sustain an oscillation. The process is illustrated in Fig. 6. Here the condition chosen corresponds to the lower left data point in Fig. 5 ($f = 0.5$ cps, $\zeta = 0.2$). The neutral stability point marked on the solid bode (corresponding to -180° phase) represents the pilot-airframe combination for a sustained oscillation. The dynamics indicated on this Bode plot are all due to the airplane, since the pilot's describing function is simply a gain. The dotted Bode represents conditions for closed-loop piloted control prior to the PIO. Here the pilot has adapted moderate lead in accordance with the closed-loop adaptation rules of Fig. 2.* The value of $1/T_L$ should be near ω_{sp}, and for convenience has been selected equal to it. Also, as always for compensatory situations with random-appearing inputs, the pilot model includes the reaction time delay term, $e^{-\tau s}$. The dotted gain line shown as appropriate to closed-loop control is set to give a phase margin of about 40° and a gain margin of about 6 db. Further, the asymptotic crossover frequency (essentially the closed-loop bandwidth) is about 1 rad/sec consistent with usual adjustment criteria.

The important point in looking at these two plots is the gain change required to go from a compensatory tracking to an oscillatory (PIO) control situation. In this case an increase of about a factor of two is required. This is not a large change as regards pilot adaptability provided the stick forces involved are not excessive. Thus, for sufficiently low stick-force gradients PIO is likely. Conversely, as the force gradient increases, the physical effort required to increase gain by a factor of two serves either to warn the pilot against this course of action or to completely prevent it (if the forces are very large).

*Incidentially, it is observed in Ref. 5 that pilot behavior in the "toe" region of Fig. 5 resembled a lead.

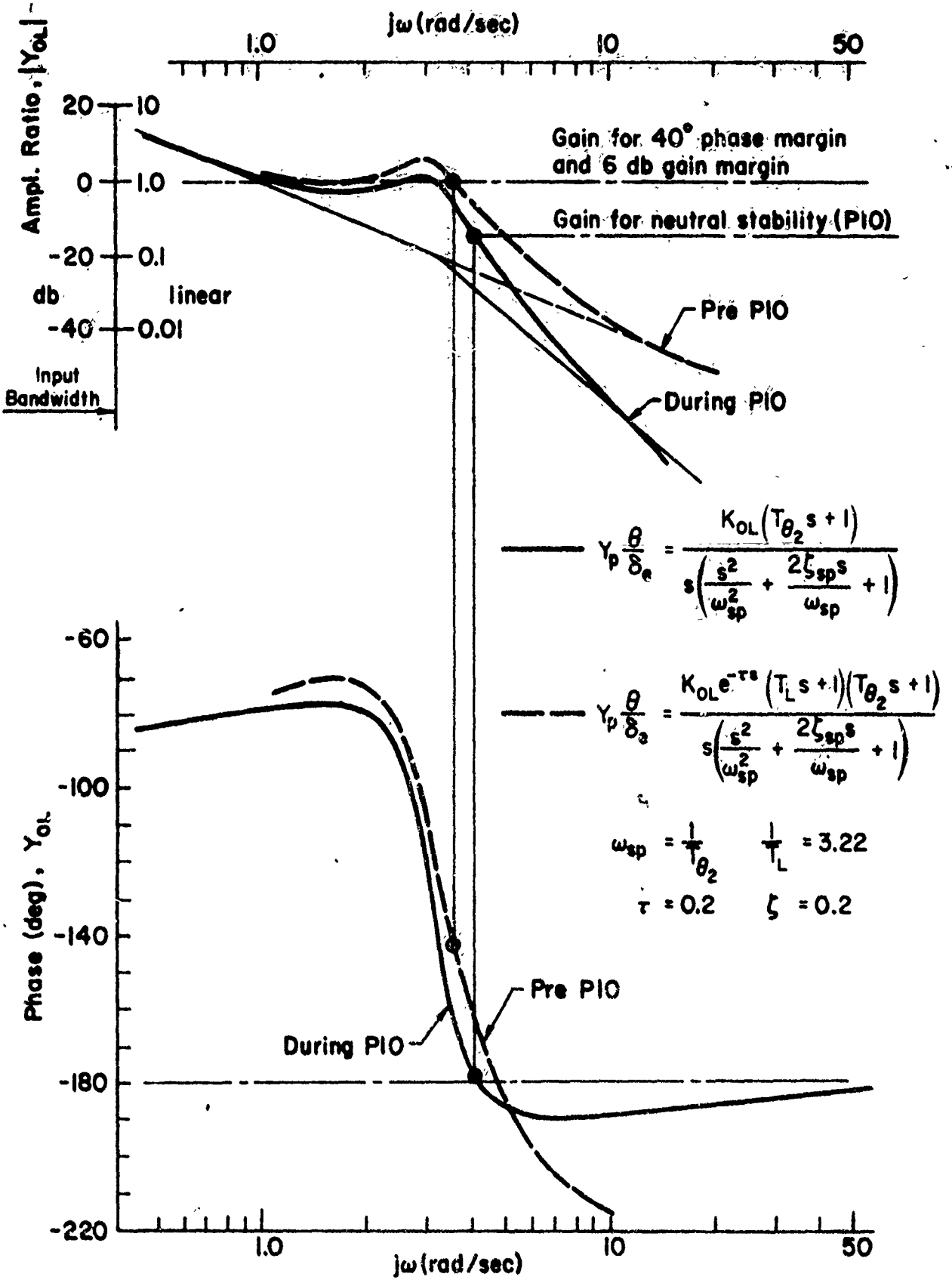

Figure 6. Bode Diagram for Pilot Control of Pitch Attitude

Although the PIO region of Fig. 5 is thus shown to be dependent on artificial relationships between $1/T_{\theta_2}$ and $\zeta_{sp}\omega_{sp}$, there <u>are</u> flight test examples of PIO's in precisely the same region (e.g., Refs. 6 and 18). The degree to which all such situations are dependent on control system or bobweight contributions, linear or nonlinear, is not precisely known. Nevertheless it appears to be true that longitudinal PIO's were non-existent (or not reported) until the advent of modern hydraulically powered elevator actuation systems. The PIO of Ref. 18 can in fact be traced directly to the <u>linear</u> contribution of the hydraulic system. That is, an analysis similar to that of Fig. 6 (including the linear contribution of the hydraulic system as measured and reported in Ref. 18) shows that the complete system is unstable at a frequency of about 5.4 rad/sec. The actual PIO record shows a basic frequency near 6 rad/sec.

As a final observation it may be concluded that, except for very unusual configurations, longitudinal attitude control PIO's can be sustained only for conditions in which control system dynamics are a contributing cause.

2. Example 2: PIO During Roll Control

For control of bank angle with aileron, the pilot-vehicle open-loop describing function for potential PIO's is given as follows, remembering that $Y_p \doteq K_p$ during a pure oscillation:

$$Y_p(s)\,\frac{\Phi}{\delta_a}(s) = \frac{K_p L'_{\delta_a}\left(s^2 + 2\zeta_\Phi\omega_\Phi s + \omega_\Phi^2\right)}{\left(s + \frac{1}{T_s}\right)\left(s + \frac{1}{T_R}\right)\left(s^2 + 2\zeta_d\omega_d s + \omega_d^2\right)} \tag{8}$$

As noted in earlier theoretical work (Refs. 9, 12, and 19) there can be a strong "ω_Φ/ω_d effect" tending to produce an oscillatory instability near Dutch roll frequency. Recent flight test examinations (Ref. 20) have confirmed this. The effect is easily seen on the generic root locus of

Fig. 7 which shows that $\omega_\phi/\omega_d > 1$ and relatively low values of ζ_d, ζ_ϕ, and ω_d are the basic requirements for a sustained oscillation. Whether or not such oscillations occur is, again, dependent on the gain differences between compensatory closed-loop control and that required to drive the system unstable. Thus, for situations in which the ω_ϕ, ω_d pair are well separated from the usual crossover frequency region (desired closed-loop bandwidth) the probability of a PIO is low, unless the damping ratio is very small ($\zeta < 0.05$) as for some high altitude aircraft. A lateral PIO can also result if some unusual forcing function requires a change in the crossover frequency. For a more complete discussion of the complex factors involved, see Ref. 12, 13 and 20.

Alternate piloting techniques can reduce the probability of these PIO's. For example, use of the rudder to damp the Dutch roll will increase both ζ_d and ζ_ϕ. The effect is to move the looped root locus connecting ω_d with ω_ϕ well into the (stable) left half-plane. Or the pilot may learn to fly at a suppressed gain level to avoid exciting the oscillation. If such techniques (or others) are required to cope with the situation, they will not be generally acceptable to pilots and will be construed as bad handling qualities (Ref. 21). Furthermore, since they are not natural and instinctive, they cannot be relied upon to prevent PIO's in emergency conditions.

The basic cure for such PIO-prone situations involves either a reduction in ω_ϕ/ω_d (by cross-feeding aileron to rudder, or by suitable augmentation driving ω_d into ω_ϕ – e.g., large roll damping) or an increase in ζ_d and ζ_ϕ (by proper feedbacks to a yaw damper).

3. Example 3: Rate-Saturated Elevator

This example considers a PIO resulting when the pilot's stick movements are faster than the maximum surface rate available from a surface servo-actuator. In a hydraulic positional servo, subjected to periodic inputs of this nature, flow-rate-limiting leads to a reduction in the ratio of surface velocity amplitude to the amplitude of the servo's oscillating error signal, thereby reducing the forward loop gain of the positional

$$Y_{OL} = \frac{K_p A_\phi \left(s^2 + 2\zeta_\phi \omega_\phi s + \omega_\phi^2\right)}{\left(s + \frac{1}{T_s}\right)\left(s + \frac{1}{T_R}\right)\left(s^2 + 2\zeta_d \omega_d s + \omega_d^2\right)}$$

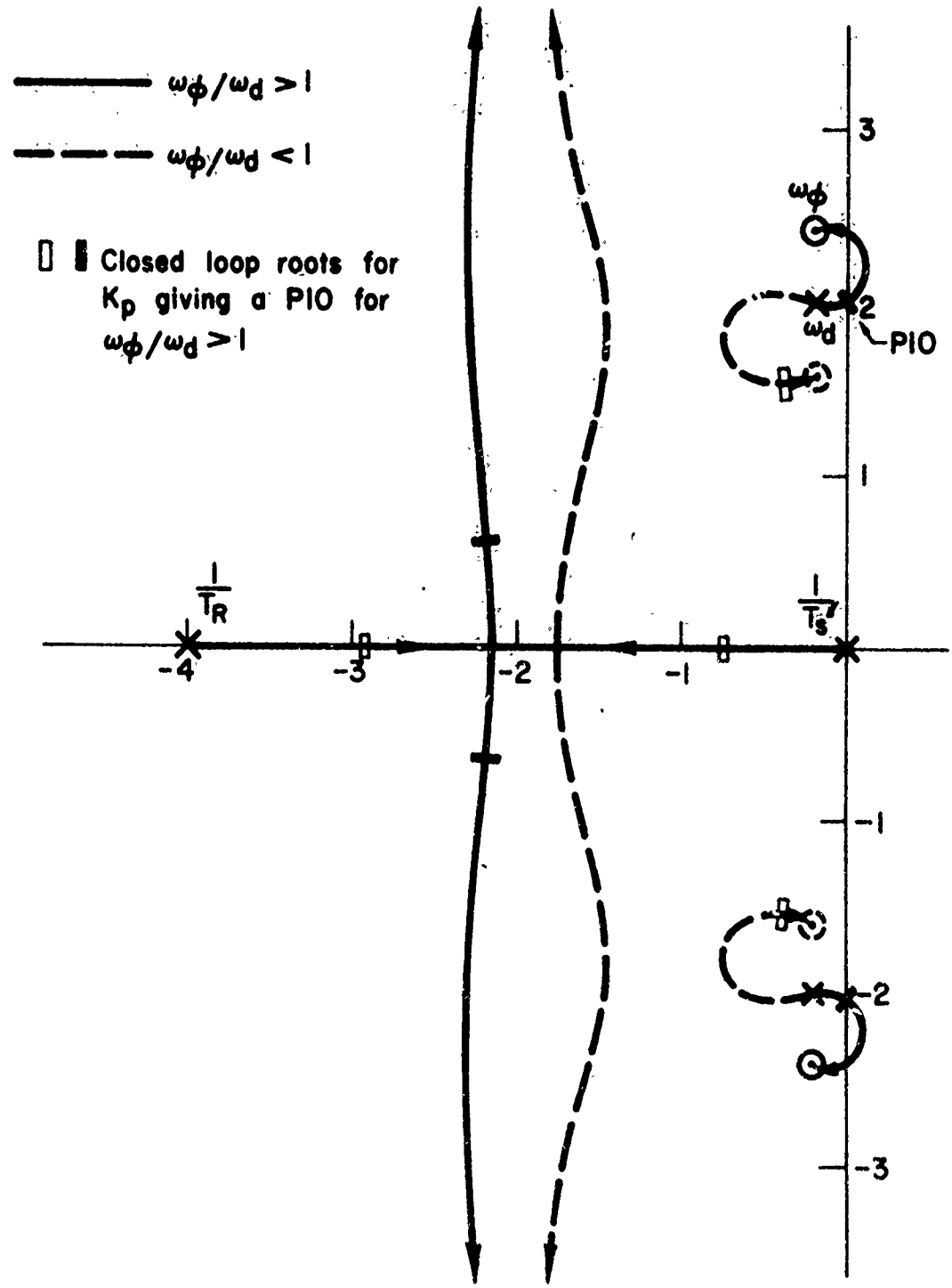

Figure 7. Root Locus Diagram for the ω_ϕ/ω_d Effect During Roll Control

servo and thus increasing its effective time constant. Qualitatively, the result is a marked degradation in the servo characteristics, effectively shifting its dynamics to lower frequencies. The major effect is an increase in the phase lag at frequencies near the pilot-vehicle system crossover. This effect, while somewhat offset by an associated attenuation increase, can still sometimes be sufficient to result in a limit cycle when large surface commands are present.

The analysis of such series nonlinearities is best done by describing function techniques, previously introduced in Section II, but in a graphical rather than analytical form.

The basic concept of describing function analysis as applied to prediction of closed-loop limit cycles (PIO) is to assume that some limit cycle exists, replace the actual waveforms around the loop with their Fourier fundamentals, and then to see if conditions are satisfied for the oscillation to be sustained. The criterion for a neutrally damped oscillation is simply that the open-loop amplitude ratio is 1.0 and the phase -180°.

When the nonlinear elements are in series, the system dynamics are separated into (a) a linear portion, represented by a frequency-dependent transfer function, $G(s)$ [or more properly $G(j\omega)$, since only sinusoids are considered]; and (b) a nonlinear portion which has transfer characteristics represented, in general, by a frequency- and amplitude-dependent describing function, $N(j\omega, A/a)$. (A/a represents the signal amplitude relative to the nonlinearity.) Then for an oscillation persist,

$$G(j\omega) \cdot N(j\omega, A/a) = -1 \tag{9}$$

or

$$G(j\omega) = \frac{-1}{N(j\omega, A/a)} \tag{10}$$

One way of using the describing function technique is to compute or measure the frequency response of the nonlinear element for a set of constant-input amplitudes, and use a conventional Bode plot to plot the total open-loop frequency response, $Y_{OL} = G \cdot N$, for each member of the set. Then the locus of intersections of the unity-amplitude-ratio points

(0 db crossovers) is projected to each corresponding phase curve, and the locus of phase margins is found. If the phase margin locus crosses the 180° line, then a limit cycle can occur at the frequency and level of input corresponding to the intersection. The stability of this limit cycle is readily determined as follows:

> The limit cycle will be stable (persist) if the phase or gain margins become more positive for increasing oscillation amplitudes, and unstable (die out or diverge) if the phase or gain margins become negative for increasing oscillation amplitudes.

A particularly simple describing function technique is possible when the describing function is dependent only on oscillation amplitude, and is independent of frequency. Making use of Eq 10, the negative inverse describing function $-1/N(A/a)$ is plotted on a standard rectangular-grid gain versus phase plot with A/a as a parameter. The linear portion, $G(j\omega)$, is also plotted on the gain-phase plot, but in the conventional fashion (i.e., using frequency as a parameter) appropriate to Nichols' chart analysis. An intersection of these two curves satisfies Eq 10 and gives the frequency and amplitude of the limit cycle. The stability of the limit cycle is given by the same criterion as before, i.e., positive gain or phase margins for increasing oscillation amplitude. This technique is used for the case at hand (see Fig. 8).

The linear transfer function plotted in Fig. 8 is that corresponding to elevator control of pitch attitude (Eq 1) for a PIO encountered on landing of the X-15 airplane (Ref. 22). The value used for the short-period frequency, $\omega_{sp} \doteq 2.3$, is based on an observed "elevator-fixed" oscillation occurring at about the same IAS as that for PIO (but about 80 sec prior to PIO onset). The values of $1/T_{\theta 2}$ and $2\zeta_{sp}\omega_{sp}$ were estimated from the basic aerodynamic data of Ref. 23 as 0.82 and 1.42, respectively. The gain used in plotting the θ/δ_e transfer function of Fig. 8 corresponds to a good linear loop closure.

Also plotted in Fig. 8 is the inverse of a simplified approximation to the describing function for the rate-limited positional servo (see the Appendix for details of its development). Two intersections of $-1/N$

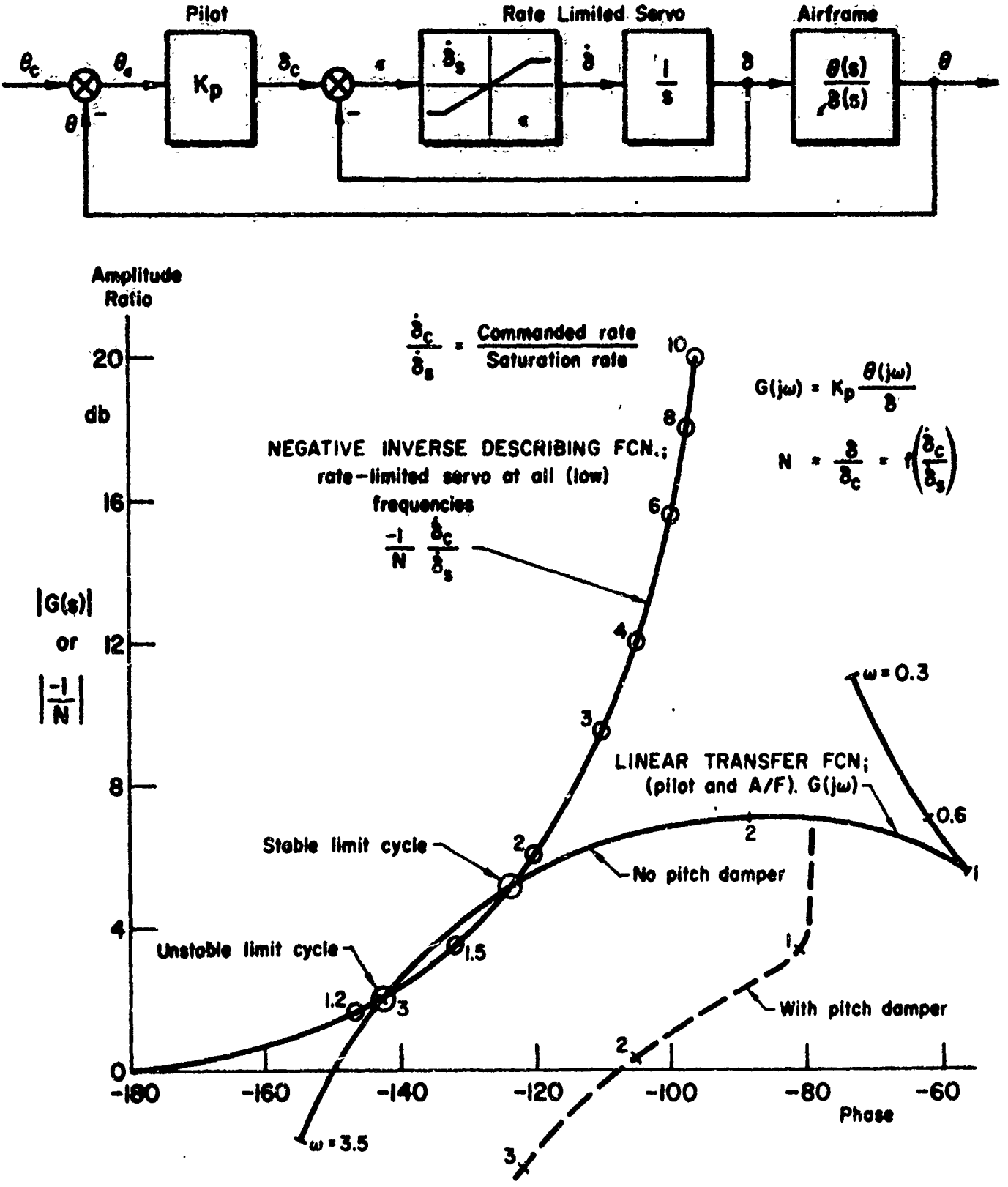

Figure 8. Gain Phase Diagram for PIO Caused by a Rate-Limited Servo

and G are present for the gain used in plotting the linear elements; a stable limit cycle is indicated at $\omega \doteq 2$, and an unstable limit cycle is at $\omega \doteq 3$. If the loop gain is slightly reduced (i.e., the entire linear plot shifted down), it would show that at the tangent point a limit cycle would start and persist at about 2.8 rad/sec, when the pilot commanded an elevator rate, $\dot{\delta}_c$, about 1.5 times the saturation rate, $\dot{\delta}_s$. Since the elevator rate is saturated for most of each cycle, the magnitude of the elevator oscillation is given by:

$$|\delta| \doteq \frac{\dot{\delta}_s}{\omega} \tag{11}$$

For the limiting elevator rate of 15°/sec used on the first X-15 flight (Ref. 24) and the theoretical frequency of 2.8 rad/sec determined above, the expected maximum value of δ_e would be ±5.3° for a total of 10.6° peak to peak. The flight test records show that at the inception of PIO (where the aerodynamics were evaluated) the period of the oscillation was about 2 sec ($\omega \doteq 3$ rad/sec) and the total elevator excursion was about 11°. This agreement between predicted and actual behavior is perhaps fortuitous in view of the simplifying assumptions made in the nonlinear analysis given in the Appendix. Nevertheless the analysis does permit a basic understanding of and appreciation for the design implications of the problem.

For example, increasing the surface velocity limits does not necessarily guarantee that PIO's will be eliminated. A change in $\dot{\delta}_s$ leaves the normalized -1/N curves of Fig. 8 completely unaltered and simply implies that to get PIO's the pilot must now move the stick at a correspondingly increased maximum rate. Since the incipient limit cycle frequency is also unchanged, this increased rate requires a larger stick position input and results in corresponding increases in the elevator deflection and airplane motions. If this rate of stick motion is difficult to attain, either inherently or because of the high stick forces required (the maximum force required to move the stick sinusoidally against a bottoming valve depends on the flexibility between the stick and valve), then the increased surface rate will probably eliminate PIO tendencies. On the other hand, if the increased stick rates are easily attained, then the PIO may be worse, i.e., of larger amplitude!

Increasing the short-period damping to 0.7, and again keeping the linear open-loop gain compatible with closed-loop considerations, gives the dashed gain-phase plot of Fig. 8. Not until the pilot's gain is raised about 8 db (a factor of 2.5) will these modified linear characteristics intersect the inverse describing function plot in limit cycle conditions described by a frequency of about 2.6 rad/sec and an $\dot{\delta}_c/\dot{\delta}_s = 2.0$. Furthermore, to sustain an oscillation requires the pilot to increase the amplitude of his input motions over those for the lower damping case by the ratios of $\dot{\delta}_c/\omega$, a factor of $(2.0/2.6)(2.8/1.5) = 1.44$. Both these influences alleviate the PIO susceptibility of the system, especially if stick-force gradients are of reasonable magnitude.

As a matter of record, the fix adopted for the X-15 PIO problem took an approach combining the various possibilities outlined above. Quoting from Ref. 24, "...it was decided by the manufacturer that (1) the less sensitive center stick would be used in subsequent landings, (2) the control-surface rate would be increased from 15 deg/sec to 25 deg/sec, (3) the longitudinal-force gradient would be increased approximately 30 percent, (4) the longitudinal breakout force would be increased slightly, and, as an additional precaution, (5) launches would be performed only if the pitch damper were operating."

4. Example 4: Nonlinear Bobweight-Friction Effects

This example is taken directly from Ref. 1, which can be consulted for more detail. It is included in the present report as an illustration treating a fairly complicated feedback nonlinearity using two sets of linearized closed-loop behavior, which correspond to the two extremes resulting from negligible or full effect of a subsidiary loop nonlinearity.

Controlled Element Characteristics. For an airplane equipped with a bobweight, the presence of friction in the control system makes the airplane's frequency response vary as a function of input force amplitude. For small stick forces resulting in small aircraft accelerations, the bobweight feedback force is too small to break through the friction band; for high forces and resulting accelerations the bobweight is full effective;

while for intermediate pilot force levels the bobweight effect varies between inactive and active states, perhaps in rapid succession. Consider as the two extremes the effective controlled element characteristics with no bobweight effect and with full bobweight effect, K_B lb/g. Then, for the system depicted in the block diagrams of Figs. 3 and 9, and the constants given in Fig. 9, the resulting $\theta/F_s(s)$ transfer functions are plotted in Bode form in Figs. 10 and 11 (note that the computation of the bobweight case requires closing the inner n_z' loop). The high altitude condition (Fig. 10) is one for which the example pilot-vehicle combination never encountered PIO problems; for the low altitude condition a very severe PIO, of about ±8g maximum amplitude, triggered the investigation of Ref. 1. The large difference in the controlled element dynamics due to the variation in the bobweight influence at low altitudes, as contrasted with the lesser variation at high altitudes, is the primary cause of the PIO tendencies in this case.

Closed-Loop Dynamics. The analysis behind this conclusion starts by considering the pilot-vehicle combination. For the low altitude, low load factor (zero effective bobweight) condition, the pilot adaptation in the frequency region of interest will be a lag. This allows him to get good crossover in a fairly extensive region of 6 db/octave slope and is consistent with the experimental evidence presented in Ref. 10. In the case at hand, a lag time constant fairly close to T_{θ_2} is desirable and, for convenience, it is assumed that $T_I = T_{\theta_2}$. The pilot model of interest here is thus simply

$$Y_p = \frac{K_p e^{-\tau s}}{(T_I s + 1)} \qquad \tau = 0.2$$

$$\frac{1}{T_I} = \frac{1}{T_{\theta_2}} = 3.18$$

and the corresponding phase and amplitude contributions result in the solid Bode plot of Fig. 12. Assuming a phase margin of 40° gives the probable gain crossover shown, resulting also in a gain margin of $K_M \doteq 4$ db. On the other hand, to sustain a large amplitude PIO (where the bobweight is fully active) requires a pure gain level corresponding

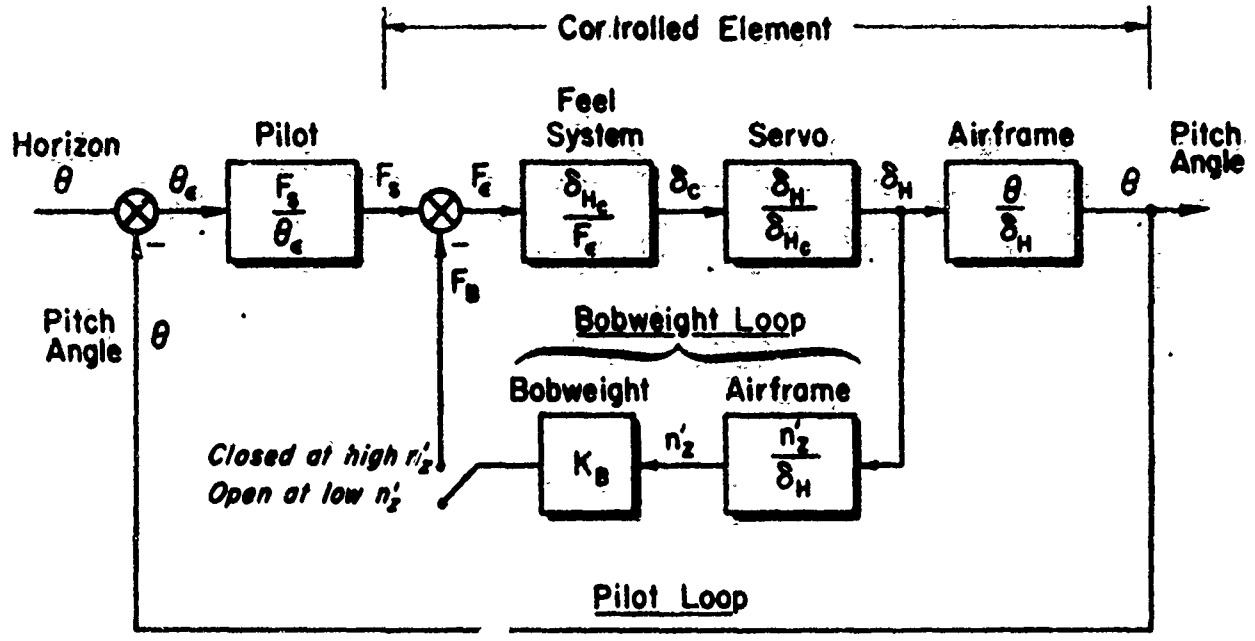

PILOT:

Pre-PIO: $\frac{F_s}{\theta_\epsilon} = \frac{K_p e^{-0.2s}}{(T_I s + 1)}$ (lb/deg)

During PIO: $\frac{F_s}{\theta_\epsilon} \doteq K_p$ (lb/deg)

FEEL SYSTEM: $\frac{\delta_c}{F_\epsilon} \doteq \frac{0.0035}{\frac{s^2}{18^2} + \frac{2(0.18)}{18} s + 1}$ (deg/lb)

SERVO: $\frac{\delta_H}{\delta_{H_c}} = \frac{1}{\frac{s}{20} + 1}$ (deg/deg)

AIRFRAME:

M = 0.85 at Sea Level	M = 0.85 at 25,000 ft
$\frac{\theta}{\delta_H} = \frac{76(s + 3.18)}{s[s^2 + 2(4)(7)s + 7^2]}$	$= \frac{20.4(s + 1.28)}{s[s^2 \quad 2(.35)(3)s + 3^2]}$
$\frac{n'_z}{\delta_H} = \frac{385}{32.2} \frac{[s^2 + 2(.17)(24.4)s + 24.4^2]}{[s^2 + 2(.4)(7)s + 7^2]}$	$= \frac{146}{32.2} \frac{[s^2 + 2(.11)(14.6)s + 14.6^2]}{[s^2 + 2(.35)(3)s + 3^2]}$ (g/de

Note: n'_z = incremental load factor at effective bobweight location

BOBWEIGHT: $K_B \doteq \begin{matrix} 0 \text{ at low } |n'_z| \\ 2.0 \text{ at high } |n'_z| \end{matrix}$ (lb/g)

Figure 9. Block Diagram and Dynamics for Analysis of Nonlinear Bobweight Friction

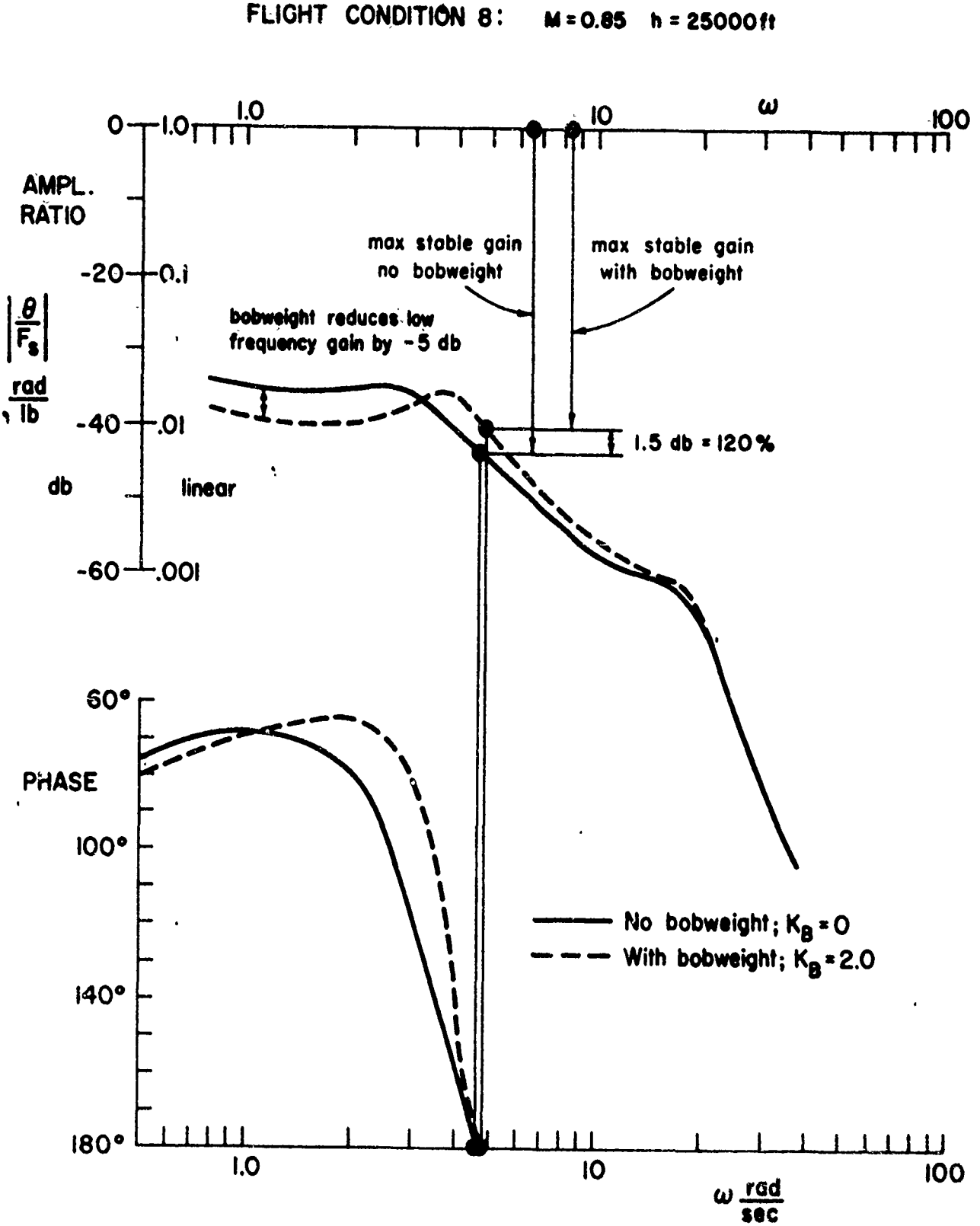

Figure 10. Effect of Bobweight on Pitch Response Away from PIO Conditions

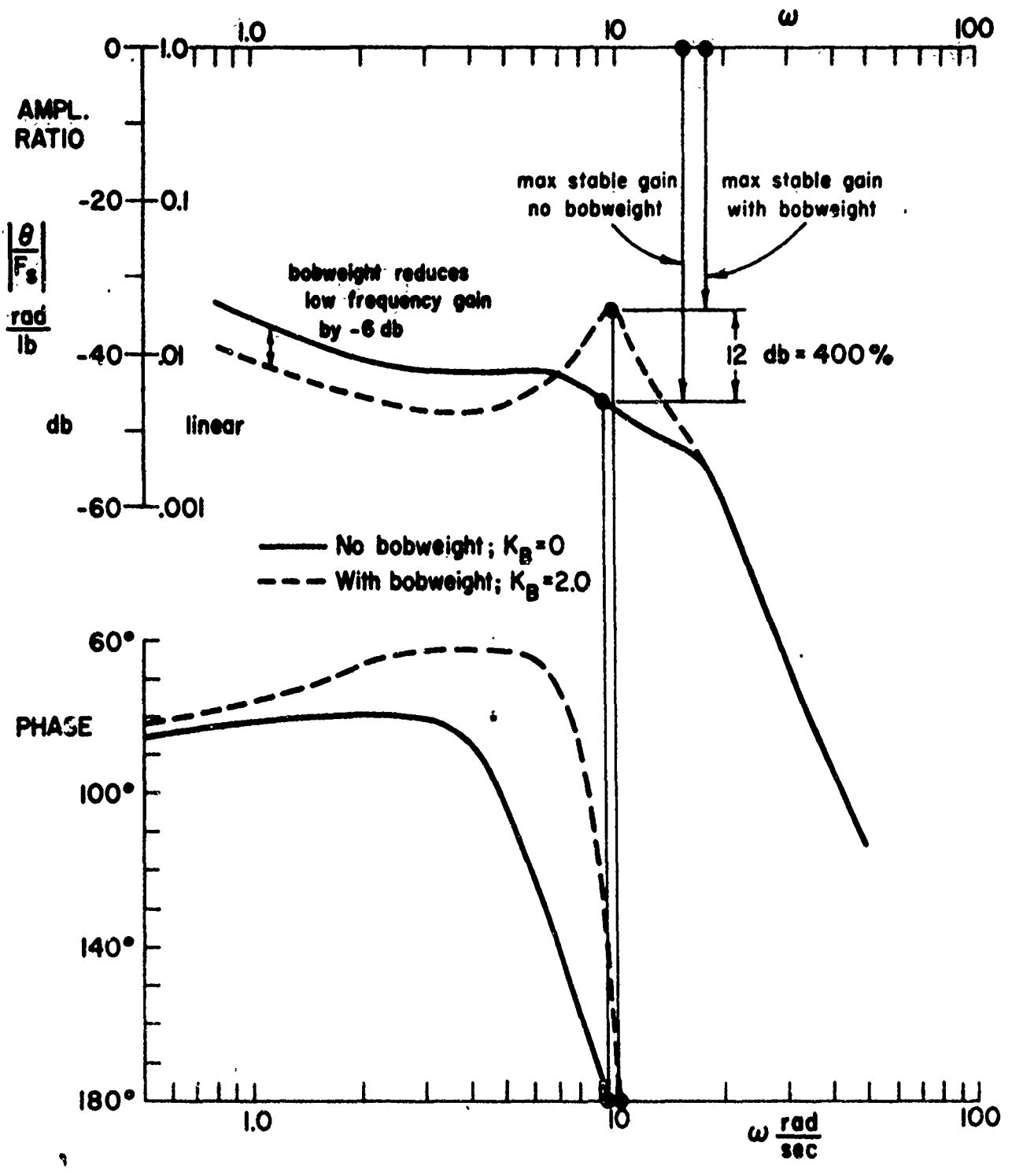

Figure 11. Effect of Bobweight on Pitch Response Near PIO Flight Conditions

——— Pre-PIO; Pilot adopts lag equalization

$$Y_{p_{opt}} = \frac{156e^{-.2s}}{\left(\frac{s}{3.2}+1\right)} \left[\frac{lb}{rad}\right] \; ; \; K_B = 0$$

— — During PIO; Pilot adopts pure gain

$$Y_p \doteq K_p \quad ; \quad K_B = 2.0$$

(K_p shown equal to pre-PIO level)

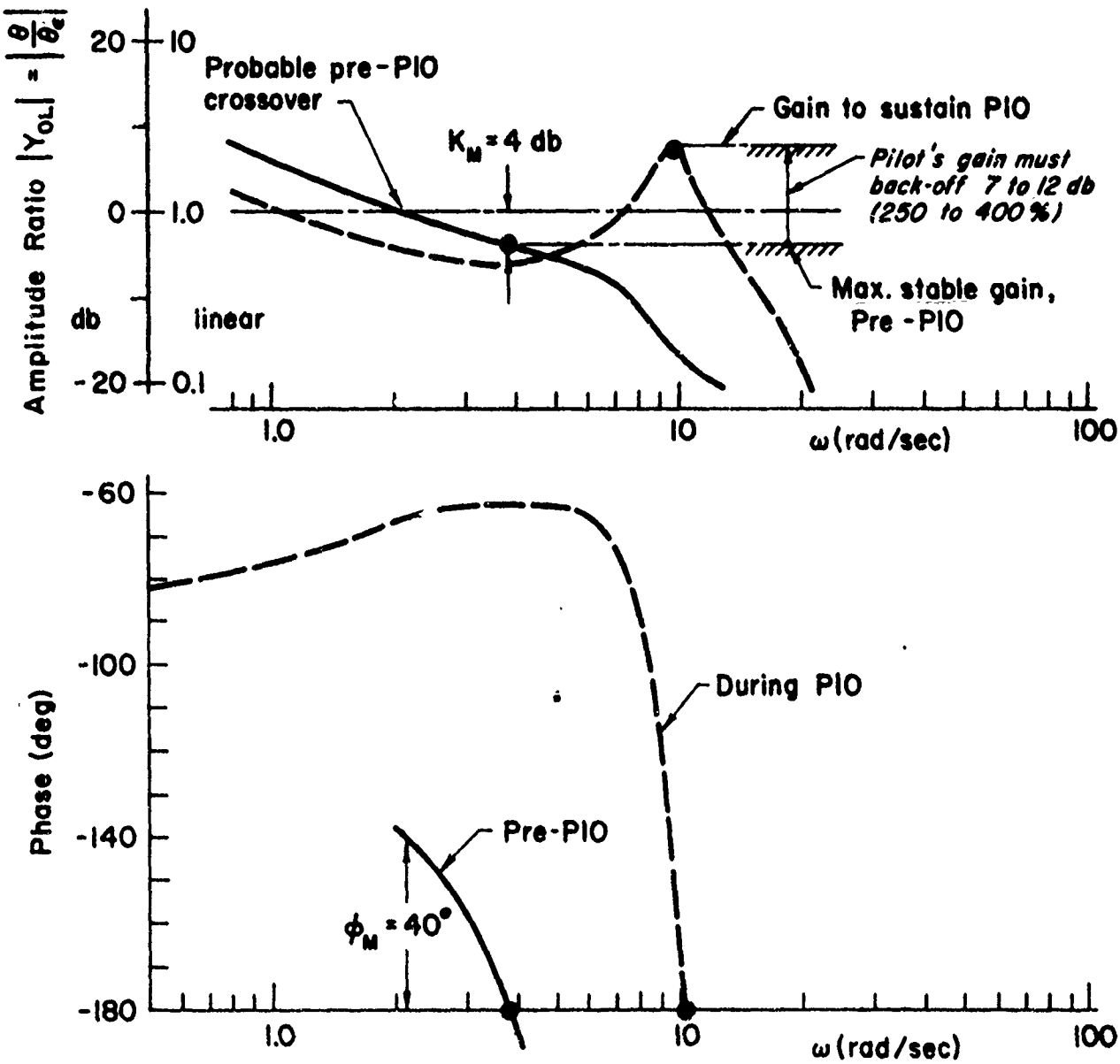

Figure 12. Comparison of Pre-PIO Pilot Loop Closure Using Lag Equalization Versus Conditions Required for a PIO When the Pilot Attempts Synchronous (Pure Gain) Behavior

to the zero phase margin of the dashed Bode. This gain level is between 7 and 12 db less than that for compensatory control! Notice also that higher gains—that is, gains closer to the compensatory level—will produce diverging oscillations. It appears, therefore, that to avoid large amplitude PIO's the pilot must reduce his gain at lease by a factor of about 3 to 4 from that normally desired (and probably used) for small precise corrections. The excessively nonlinear and rapid readaptation required of the pilot to avoid PIO is more than the pilot can accommodate. Also, the basic characteristics with the bobweight active ($\omega'_{sp} = 9.8$, $\zeta'_{sp} = 0.10$, $1/T_{\theta_2} = 3.18$) are themselves quite poor (Ref. 5), and even if there were no nonlinear action due to friction the system would probably be PIO prone in the sense of Example 1 (i.e., $2\zeta'_{sp}\omega'_{sp} - 1/T_{\theta_2} = -1.2$).

Cure. The basic cure lies in removing the peak in the bobweight-augmented response while preserving the low frequency stick-force-per-g characteristics desired at this flight condition. This is done most simply by reducing the bobweight loop gain by a factor of 2 to 4 while preserving low frequency stick-force-per-g characteristics required by specifications. This is feasible because the pilot loop gain involves the quotient of K_B/K_F (where K_F is the feel spring gradient: $K_F = F_s/\delta_{H_c}$), while the static stick force per g involves the sum of $K_B + (K_F \cdot \text{constant})$. The bobweight gain was reduced from $K_B = 2.0$ to 1.0 lb/g, while the feel spring gradient was increased (for small stick deflections) from $K_F = 5$ to 10 lb/in. The resulting loop gains and stick-force-per-g parameters are shown in Table III. Whereas the original T-38A bobweight

TABLE III

COMPARISON OF BASIC AND MODIFIED PARAMETERS

	Basic T-38A		Modified T-38A
Bobweight gain, lb/g.....	0	2.0 (max)	1.0 (max)
Feel spring gradient, lb/in.....	5.0	5.0	10.0
Gearing, deg/in.....	1.05	1.05	1.05
Inner loop gain at PIO conditions, F_B/F_ϵ.....	0	1.0	0.25
Static stick force per g, lb/g.....	2.0	4.0	4.6
Minimum dynamic stick force per g, lb/g.....	1.2	0.7	2.9

characteristics resulted in a drop-off in stick force per g from 4.0 to 0.7 lb/g near the PIO frequency, the modified characteristics only drop from 4.6 to 2.9 lb/g in this frequency region. It is also apparent that the original unaugmented airframe had overly sensitive static stick-force-per-g characteristics. It is felt that the bobweight loop gain reduction of 400 percent is about the minimum which will result in elimination of the basic PIO tendencies, although lesser percentages would certainly result in substantial improvement.

The consequences of increasing the feel spring gradient in conjunction with reducing the bobweight gain yield a twofold benefit:

1. The bobweight loop gain is reduced as K_p is increased.
2. The feel system frequency, ω_F, is increased by the square root of the change in K_F, i.e., from 18 to 25 rad/sec, which moves it farther away from the short-period frequency and reduces its adverse effect on the coupled short-period damping ratio.

Increasing K_F has some serious disadvantages, however. Since the bobweight influence is reduced, the static stick force per g is more affected by variations in the flight conditions, so F_s/g will not be as constant over the entire flight envelope as in the basic design. Furthermore, the increased force gradient may result in excessive maximum stick forces during landing, takeoff, or supersonic conditions when large stick deflections are required. Thus, the cure for the PIO tendencies will perhaps detract from the general airplane handling qualities taken across the entire flight regime.

Optimum Recovery Technique. This analysis also reveals the optimum technique for rapid recovery from a pilot-induced oscillation of this type. If a PIO is started, it can be stopped either by releasing the stick or by clamping it securely, i.e., opening the loop. Clamping the stick will cause the oscillation to decay at the stick-fixed short-period damping ratio ($\zeta_{sp} \doteq 0.4$), whereas releasing the stick will cause the oscillation to decay at the stick-free short-period damping ratio ($\zeta'_{sp} \doteq 0.1$). Since ζ'_{sp} is always less than ζ_{sp}, the best recovery procedure theoretically

is to clamp the stick securely. For the unmodified T-38A, this should damp the oscillations roughly 2 to 4 times as fast as releasing the stick, depending on the amount of stick friction. However, if it is difficult to achieve rigid clamping during a violent PIO, then releasing the stick is the only alternative.

Summary. In summary, it is concluded that at low altitude, high subsonic flight conditions the airframe sensitivity to stick forces is sufficiently high that bobweight effects can produce marginally stable stick-free short-period characteristics at large load factors. At low load factors control system friction prevents bobweight feedback. When large stick inputs result in high load factors, the full effect of the bobweight interactions are felt, and the pilot must reduce his gain severalfold to avoid a pilot-induced oscillation. To stop a developed PIO, clamping the stick is theoretically more effective than simply releasing the stick. At high altitude conditions, the difference in tolerable pilot gain for instability due to bobweight effects is negligible, and no PIO is induced. The simplest recommended cure consists of increasing the feel system spring gradient for small stick deflections while decreasing the bobweight gain.

5. Concluding Remarks

The wide range of PIO problem areas, physical causes, analysis techniques, and cures illustrated in the preceding examples shows that pat prescriptions for PIO causes, analyses, and cures are not to be expected. Each case must be treated individually and thoroughly, and competing fixes should be evolved before a decision as to the best is made. The hopeful note in all this complexity is the demonstration herein that well-known analytical techniques, combined with recent data on the human pilot's behavior (both prior to and during a PIO) and system describing function data in the proper detail, can correctly assess the basic causes of pilot-induced oscillations and reveal the most promising cures.

REFERENCES

1. Jex, H. R., Summary of T-38A PIO Analyses, Systems Technology, Inc., TR-239-1, January 1963.

2. Abzug, Malcolm J., High-Speed Stability and Control Problems as They Affect Flight Testing, AGARD Rept. 120, May 1957.

3. Phillips, William H., B. Porter Brown, and James T. Matthews, Jr., Review and Investigation of Unsatisfactory Control Characteristics Involving Instability of Pilot-Airplane Combination and Methods for Predicting These Difficulties from Ground Tests, NACA TN 4064, August 1957.

4. Nelson, W. E., and O. A. Levi, An Analytical and Flight Test Approach to the Reduction of Pilot Induced Oscillation Susceptibility, Northrop-Norair Division Rept., October 1963.

5. A'Harrah, R. C., and R. P. Schulze, An Investigation of Low-Altitude High Speed Flying and Riding Qualities of Aircraft, North American Aviation, Inc., Rept. NA-62H-397, February 1963.

6. Richardson, J. D., and R. C. A'Harrah, The Application of Flight Simulators to the Development of the A-5A Vigilante, paper presented at AIAA Simulation for Aerospace Flight, National Specialists Meeting, August 1963.

7. Terrill, W. H., L. R. Springer, and J. G. Wong, Investigation of Pilot-Induced Longitudinal Oscillation in the Douglas Model A4D-2 Airplane, Douglas Aircraft Company, Inc., Rept. LB-25452, May 15, 1957. (CONFIDENTIAL report)

8. Decker, James L., "The Human Pilot and the High-Speed Airplane," J. Aeron. Sc., Vol. 25, No. 8, August 1956, pp. 765-770.

9. Ashkenas, I. L., and Duane T. McRuer, The Determination of Lateral Handling Quality Requirements from Airframe-Human Pilot System Studies, WADD TR-59-135, June 1959.

10. McRuer, Duane T., Irving L. Ashkenas, and C. L. Guerre, A Systems Analysis View of Longitudinal Flying Qualities, WADD TR-60-43, January 1960.

11. Jex, H. R., and C. H. Cromwell, III, Theoretical and Experimental Investigation of Some New Longitudinal Handling Qualities Parameters, ASD-TR-61-26, June 1962.

12. Durand, T. S., and H. R. Jex, Handling Qualities in Single-Loop Roll Tracking Tasks: Theory and Simulator Experiments, ASD-TDR-62-507, November 1962.

13. Ashkenas, I. L., and D. T. McRuer, "A Theory of Handling Qualities Derived from Pilot-Vehicle System Considerations," Aerospace Engineering, Vol. 21, No. 2, February 1962.

14. McRuer, D. T., and E. S. Krendel, "The Man-Machine System Concept," Proc. IRE, Vol. 50, No. 5, May 1962.

15. Graham, Dunstan, and Duane McRuer, Analysis of Nonlinear Control Systems, John Wiley and Sons, Inc., New York, 1961.

16. McRuer, Duane, and Dunstan Graham, Pilot-Vehicle Control Systems Analysis, AIAA Paper 63-310, August 1963.

17. Ashkenas, Irving L., and Duane T. McRuer, Approximate Airframe Transfer Functions and Applications to Single Sensor Control Systems, WADC TR-58-82, June 1958.

18. McFadden, Norman M., Frank A. Pauli, and Donovan R. Heinle, A Flight Study of Longitudinal-Control-System Dynamic Characteristics by the Use of a Variable-Control-System Airplane, NACA RM A57L10, March 1958.

19. Ashkenas, I. L., and D. T. McRuer, "Optimization of the Flight-Control, Airframe System," J. Aero/Space Sc., Vol. 27, No. 3, March 1960.

20. Taylor, Lawrence W., Jr., Analysis of a Pilot-Airplane Lateral Instability Experienced with the X-15 Airplane, NASA TN D-1059, November 1961.

21. Harper, Robert P., Jr., In-Flight Simulation of the Lateral-Directional Handling Qualities of Entry Vehicles, WADD TR-61-147, February 1961.

22. Finch, Thomas W., and Gene J. Matranga, Launch, Low-Speed, and Landing Characteristics Determined from the First Flight of the North American X-15 Research Airplane, NASA TM X-195, September 1959.

23. Lopez, Armando E., and Bruce E. Tinling, The Static and Dynamic-Rotary Stability Derivatives at Subsonic Speeds of a Model of the X-15 Research Airplane, NACA RM A58F09, September 1958.

24. Matranga, Gene J., Analysis of X-15 Landing Approach and Flare Characteristics Determined from the First 30 Flights, NASA TN D-1057, July 1961.

25. Synopsis of the Current STI-FI Pilot-Vehicle Response Program, and Highlights of Pilot-Vehicle Response Program, Systems Technology, Inc., WP-134-7 and WP-134-8, 28 February 1964.

26. Final Report: Human Dynamic Study, Goodyear Aircraft Corp. Rept. GER-4750, April 8, 1952.

27. Mayne, Robert, Some Engineering Aspects of the Mechanism of Body Control, Goodyear Aircraft Corp. Rept. GER-2435, December 18, 1950. (See also: Mayne, Robert, "Some Engineering Aspects of the Mechanism of Body Control," Electrical Engineering, Vol. 70, No. 3, March 1951.)

28. Ellson, Jerome I., and F. Gray, Frequency Responses of Human Operators Following a Sine Wave Input, USAF AMC Memo Rept. MCREXD-694-2N, 1948.

29. Krendel, Ezra S., and Duane T. McRuer, "A Servomechanisms Approach to Skill Development," J. Franklin Inst., Vol. 269, No. 1, January 1960, pp. 24-42.

30. Stark, Lawrence, Mitsuo Iida, and Paul A. Willis, "Dynamic Characteristics of the Motor Coordination System in Man," Biophysical J., Vol. 1, 1961, pp. 279-300.

31. Muckler, F. A., R. O. Hcokway, and H. H. Burke, "Manned Control of Large Space Boosters," Trans. Seventh Symposium on Ballistic Missiles and Space Technology, 13-16 August 1962, Vol. II, p. 176.

32. Archer, Donald D., and Charles L. Gandy, Jr., T-37A Phase IV Performance and Stability and Control, AFFTC-TR-56-37, February 1957.

33. Crawford, Charles C., and Jones P. Seigler, KC-135A Stability and Control Test, AFFTC-TR-58-13, May 1958.

34. Simmons, Carl D., and Donald M. Sorlie, F-101B Air Force Stability and Control Evaluation, AFFTC-TR-58-11, May 1958.

35. Grosso, Vincent A., An Investigation to Determine the Effects of Several Parameters on Optimum Zoom Climb Performance, AFFTC-TN-59-32, September 1959.

36. Allender, J. Reverdy, and Robert M. White, F-102A Phase IV Stability Test, AFFTC-TR-57-5, April 1957.

37. Phillips, William H., B. Porter Brown, and James T. Matthews, Review and Investigation of Unsatisfactory Control Characteristics Involving Instability of Pilot-Airplane Combination and Methods for Predicting These Difficulties from Ground Tests, NACA TN 4064, August 1957

38. Seckel, Edward, Ian A.M. Hall, Duane T. McRuer, and David H. Weir, Human Pilot Dynamic Response in Flight and Simulator, WADC-TR-57-520, August 1958.

39. Newell, Fred, Investigation of Phugoid Effects on GCA Landings, WADC-TR-57-650, December 1957.

APPENDIX

DERIVATION OF THE DESCRIBING FUNCTION FOR A RATE-SATURATED POSITIONAL SERVO

The rate-limited servo is described by the following block diagram and parameters:

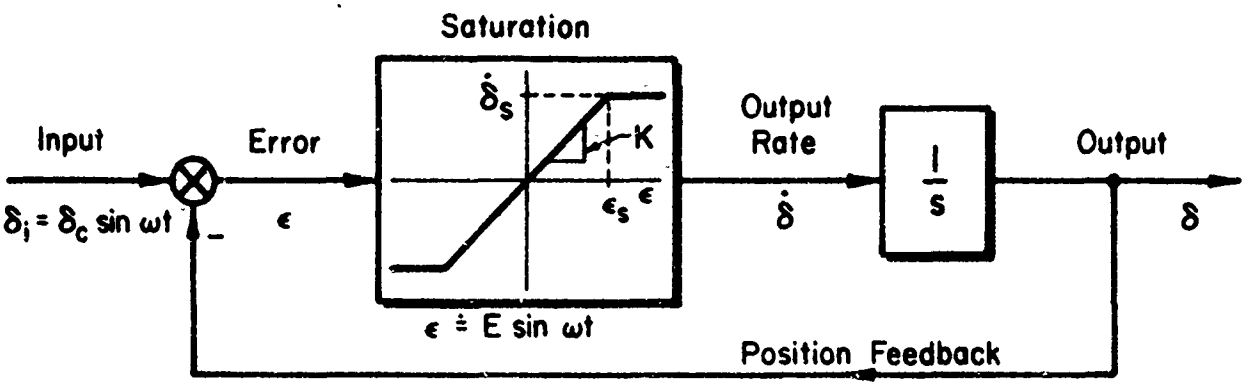

The output rate is proportional to the error with gain K for errors less than ϵ_s, but is saturated at a level $\dot{\delta}_s$ for error signals larger than ϵ_s. The problem in determining the closed-loop sinusoidal describing function, δ/δ_c, is that the error signal is not sinusoidal when the rate exceeds saturation, and it is not simply related to the input, as it is for linear operation. A numerical or graphical cross-plotting scheme, such as that described in Ref. 15, pp. 209 ff., could be used to obtain an "exact" describing function for δ/δ_c. A simpler analytical approximation is used herein which reveals all the essential features with sufficient accuracy for most practical problems.

The error signal is assumed to be closely represented by a pure sinusoid of amplitude E: $\epsilon = E \sin(\omega t + \varphi)$. The sinusoidal describing function for the limiter itself is well known (e.g., Ref. 15, pp. 106, 110, 114, 129, 238). For $E > \epsilon_s$ the amplitudes of the Fourier fundamental of the output is given in terms of the input to the nonlinearity by

$$b_1 = \frac{2E}{\pi}\left[\sin^{-1}\frac{\epsilon_s}{E} + \frac{\epsilon_s}{E}\sqrt{1 - \frac{\epsilon_s^2}{E}}\right]; \quad E > \epsilon_s \qquad \text{(A-1)}$$

The effective gain of the nonlinearity is

$$K' = K \quad \text{for} \quad E \leq \epsilon_s \tag{A-2}$$

$$K' = \frac{b_1}{E} \quad \text{for} \quad E > \epsilon_s \tag{A-3}$$

This relationship, as a function of E/ϵ_s, is shown in Fig. A-1, normalized with respect to the linear gain, K. Also shown are two approximations to the saturated describing function:

1. The upper approximation is asymptotically correct at large error amplitudes where the output rate looks like a square wave (whose fundamental amplitude is $4/\pi$ times the saturation rate). For this case,

$$K' \doteq \frac{4}{\pi}\frac{\dot{\delta}_s}{E} \; ; \; \frac{E}{\epsilon_s} \gg \frac{4}{\pi} \tag{A-4}$$

2. The lower approximation curve is asymptotically correct at errors just exceeding the saturation point, where the slightly clipped output still looks like a sinusoid whose amplitude is approximated by the saturation rate itself, $\dot{\delta}_s$, instead of the Fourier fundamental of Eq A-1.

$$K' \doteq \frac{\dot{\delta}_s}{E} \; ; \; \frac{E}{\epsilon_s} \rightarrow 1.0^+ \tag{A-5}$$

It is apparent from Fig. A-1 that the approximation of Eq A-4 is actually very good for $E/\epsilon_s > 2.0$, and is about as good as Eq A-5 for $1.0^+ < E/\epsilon_s < 2.0$. Nevertheless, Eq A-5 is simpler to handle and still reveals the essential features of the closed-loop system.

The error amplitude, E, must now be related to the command, δ_c. From fundamental closed-loop relationships we have

$$Y_\epsilon(s) = \frac{\epsilon(s)}{\delta_i(s)} = \frac{1}{1 + Y_{OL}(s)} \; ; \; Y_{OL} = \frac{K'}{s} \tag{A-6}$$

and replacing s by $j\omega$ for a pure sinusoidal input gives

$$\frac{\epsilon(j\omega)}{\delta_i(j\omega)} = \frac{1}{1 + K'/j\omega}$$

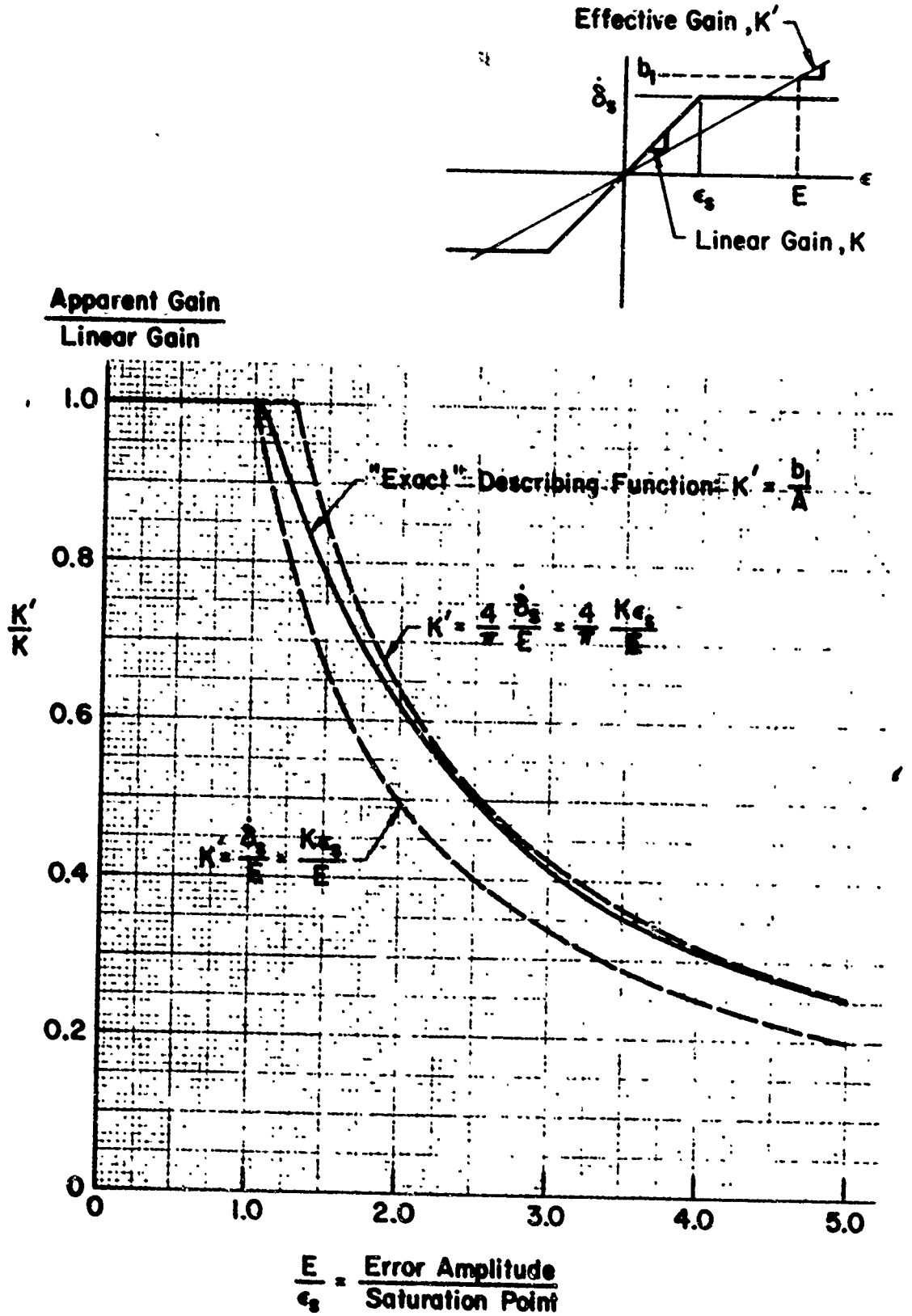

Figure A-1. Sinusoidal-Input Describing Function for the Limiting Element

Carrying out the algebra, remembering that $j^2 = -1$, and solving for the magnitude of the complex quantities, we get

$$\frac{|\epsilon(j\omega)|}{|\delta_i(j\omega)|} = \frac{E}{\delta_c} = \frac{\omega}{\left[\omega^2 + (K')^2\right]^{1/2}} \qquad \text{(A-7)}$$

where δ_c is the maximum command displacement input. At this point K' is still dependent on E in general, but choosing one of the approximations of Eq A-4 or A-5 removes this dependence (for $E > \epsilon_s$) and is the analytical key to a simple solution. Equation A-7 may then be manipulated algebraically to yield expressions for $|E/\epsilon_s|$ and thus for $|E/\dot{\delta}_s|$ and hence K', in terms of the command instead of the error. The results of this, using the simpler expressions of Eq A-5, are:

$$K' \doteq \frac{\dot{\delta}_s}{E} = \frac{K\epsilon_s}{E} \quad ; \quad \frac{E}{\epsilon_s} \rightarrow 1.0^+ \qquad \text{(A-8)}$$

$$\frac{E}{\epsilon_s} = \left[\left(\frac{\delta_c}{\epsilon_s}\right)^2 - \left(\frac{K}{\omega}\right)^2\right]^{1/2} \quad ; \quad \frac{E}{\epsilon_s} \rightarrow 1.0^+ \qquad \text{(A-9)}$$

$$\frac{E}{\dot{\delta}_s} = \left[\left(\frac{\delta_c}{\dot{\delta}_s}\right)^2 - \left(\frac{1}{\omega}\right)^2\right]^{1/2} \quad ; \quad \frac{E}{\dot{\delta}_s} \rightarrow \frac{1}{K}^+ \qquad \text{(A-10)}$$

Therefore,

$$K' \doteq \frac{1}{\left[\left(\frac{\delta_c}{\dot{\delta}_s}\right)^2 - \left(\frac{1}{\omega}\right)^2\right]^{1/2}} \quad ; \quad \frac{\dot{\delta}_s}{E} \rightarrow K^- \qquad \text{(A-11)}$$

The closed-loop response can now be determined from the basic relationship for Y_{CL}:

$$Y_{CL} = \frac{\delta}{\delta_c} = \frac{Y_{OL}}{1 + Y_{OL}} = \frac{1}{\frac{1}{K'}s + 1} = \frac{1}{Ts + 1} \qquad \text{(A-12)}$$

For the linear range of operation ($E/\epsilon_s \leq 1.0$) this is just a first-order lag given as $T \equiv 1/K$, which increases as K' becomes less than K beyond the saturation level.

Putting $s = j\omega$ and substituting Eq A-11 for $1/K'$ gives

$$Y_{CL} = \frac{\delta(j\omega)}{\delta_c(j\omega)} = \frac{1}{j\frac{\omega}{K'} + 1} \quad ; \quad \frac{E}{\epsilon_s} \rightarrow 1.0^+$$

$$= \frac{1}{\left[\left(\frac{\delta_c\omega}{\dot{\delta}_s}\right)^2 - 1\right]^{1/2} j + 1} \qquad \text{(A-13)}$$

Thus, at constant input amplitude, the closed-loop describing function depends on both amplitude and frequency once saturation occurs. However, recognizing that the input rate for a sinusoid is just $\dot{\delta}_c = \delta_c\omega$, Eq A-13 may be simplified further to eliminate the frequency dependence:

$$Y_{CL} = \frac{1}{\left[\left(\frac{\dot{\delta}_c}{\dot{\delta}_s}\right)^2 - 1\right]^{1/2} j + 1} \qquad \text{(A-14)}$$

The associated gain and phase are given by

$$|Y_{CL}| = \frac{1}{\left[\left(\frac{\dot{\delta}_c}{\dot{\delta}_s}\right)^2 - 1 + 1\right]^{1/2}} = \frac{\dot{\delta}_s}{\dot{\delta}_c} \quad ; \quad \frac{E}{\epsilon_s} \rightarrow 1.0^+ \qquad \text{(A-15)}$$

$$\not\propto Y_c = -\tan^{-1}\sqrt{\left(\frac{\dot{\delta}_c}{\dot{\delta}_s}\right)^2 - 1} \quad ; \quad \frac{E}{\epsilon_s} \rightarrow 1.0^+ \qquad \text{(A-16)}$$

Since Eq A-9 is asymptotically correct at the saturation point, we can solve it for ω_s at saturation ($E/\epsilon_s = 1.0$), giving

$$\omega_s \geq \frac{K}{\left[\left(\frac{\delta_c K}{\dot{\delta}_s}\right)^2 - 1\right]^{1/2}} \qquad \text{(A-17)}$$

which, by further algebra and with $\dot{\delta}_c = \delta_c \omega$, may be put in the form

$$\left(\frac{\delta_c}{\dot{\delta}_s}\right)^2\Bigg|_s \geq 1 + \frac{\omega^2}{K^2} \tag{A-18}$$

The meaning of this is as follows: K is the linear closed-loop break frequency of the servo and is a large value like 20 to 50 rad/sec. The input frequencies, ω, are rather low, usually less than 10 rad/sec. Hence, $\omega^2/K^2 \ll 1$ for practical problems, and the saturation criterion reduces to the simple statement that the maximum commanded rate exceeds the output rate limit. This is not surprising, since the output is closely following the commands at low frequencies; hence the output rate starts saturating when the command rate reaches the saturation value. Equation A-18 shows that at higher frequencies (comparable with the servo break frequency, K) more command rate is required to saturate the servo.

Expressions similar to Eq A-8 through A-18 result for the asymptotic approximation of Eq A-4, with the constant $4/\pi = 1.27$ appearing in several places. All possible forms are summarized below.

Linear range:

$$Y_{CL} = \frac{\delta(j\omega)}{\delta_c(j\omega)} = \frac{1}{\frac{j\omega}{K} + 1} \quad \text{for} \quad \omega < \omega_s \quad \text{or} \quad \dot{\delta}_c < \dot{\delta}_s$$

$$|Y_{CL}| = \left(\frac{\omega^2}{K^2} + 1\right)^{-1/2} \tag{A-19}$$

$$\measuredangle Y_{CL} = -\tan^{-1}\frac{\omega}{K}$$

Saturation:

Saturation frequency:

$$\omega_s = \frac{K}{\sqrt{\left(\frac{\dot{\delta}_c K}{\dot{\delta}_s}\right)^2 - 1}} \quad \text{or} \quad \frac{K}{\sqrt{\left(\frac{\delta_c}{\epsilon_s}\right)^2 - 1}} \tag{A-20}$$

For $E/\epsilon_s \quad 1.0^+$ ($\dot{\delta}_c/\dot{\delta}_s \quad 1.0^+$); Small saturation:

$$|Y_{CL}| \doteq \frac{\dot{\delta}_s}{\delta_c \omega} \text{ or } \frac{\dot{\delta}_s}{\dot{\delta}_c}$$

$$\not\propto Y_{CL} \doteq -\tan^{-1}\sqrt{\left(\frac{\delta_c \omega}{\dot{\delta}_s}\right)^2 - 1}$$

or

$$-\tan^{-1}\sqrt{\frac{\dot{\delta}_c^2}{\dot{\delta}_s^2} - 1} \qquad \text{(A-21)}$$

For $E/\epsilon_s \gg 1.0$ ($\dot{\delta}_c/\dot{\delta}_s \gg 1.0$); Large saturation:

$$|Y_{CL}| \doteq \frac{4}{\pi}\frac{\dot{\delta}_s}{\delta_c \omega} \text{ or } \frac{4}{\pi}\frac{\dot{\delta}_s}{\dot{\delta}_c}$$

$$\not\propto Y_{CL} \doteq -\tan^{-1}\sqrt{\left(\frac{\pi}{4}\frac{\delta_c \omega}{\dot{\delta}_s}\right)^2 - 1}$$

or

$$-\tan^{-1}\sqrt{\left(\frac{\pi}{4}\frac{\dot{\delta}_c}{\dot{\delta}_s}\right)^2 - 1} \qquad \text{(A-22)}$$

The resulting approximate describing functions, $N(j\omega, \dot{\delta}_c/\dot{\delta}_s)$, are given in Table A-I for various values of $\dot{\delta}_c/\dot{\delta}_s$, while in Fig. A-2 the negative inverse describing functions, $-1/N$, are plotted on a log-gain-phase plot. The gain phase diagram (Nichols Chart) facilitates limit cycle analyses when the describing function depends only on a relative amplitude parameter, and not on frequency. Actually, the complete describing function for the rate-limited servo consists of three parts: a linear portion below saturation which depends only on frequency (first-order lag with break frequency = K); a second small portion which depends on amplitude, $\dot{\delta}_c/\dot{\delta}_s$, and applies for $E/\epsilon_s \approx 1.0^+$; this blends into

TABLE A-I

DESCRIBING FUNCTION FOR A RATE-SATURATED POSITION SERVO

$$N = \frac{\delta}{\delta_c} = f\frac{\dot{\delta}_c}{\dot{\delta}_s}$$

|N|		∠ N (Deg)	FOR LINEAR OPERATION $\frac{E}{\epsilon_s} < 1$	FOR SMALL SATURATION $\frac{E}{\epsilon_s} \doteq 1$	FOR LARGE SATURATION $\frac{E}{\epsilon_s} \gg \frac{4}{\pi}$
Linear	db		ω/K	$\dot{\delta}_c/\dot{\delta}_s$	$\dot{\delta}_c/\dot{\delta}_s$
1	0	0	0	1	——
0.833	-1.5	-33.5	0.663	1.2	——
0.787	-2	-38	0.783	1.27	1
0.707	-3	-45	1.00	1.414	1.11
0.625	-4	-51.3	1.25	1.6	1.26
0.5	-6	-60	1.732	2	1.57
0.333	-9.5	-70.5	2.83	3	2.36
0.25	-12	-75.5	3.87	4	3.14
0.2	-14	-78.5	4.9	5	3.93
0.1	-20	-84.25	9.95	10	7.87
0	$-\infty$	-90	∞	∞	∞

a third portion, beyond $E/\epsilon_s \doteq 2$, also dependent only on amplitude. As shown in Fig. A-2, when plotted on a gain phase diagram, all three portions lie along one curve. (The linear portion has frequency as a parameter with the break frequency $\omega = 1/T = K$ at $|-1/N| = 3$ db and $\angle -1/N = 135°$.)

Neutral stability of the linear portion occurs when the $G(j\omega)$ curve intersects the $-1/N$ curve **at the same frequency,** and it will be assumed that positive gain and phase margins exist for linear operation (small commands). The nonlinear portion then becomes, to first-order accuracy, dependent only on the relative amplitude of command rate to saturation

rate of the position servo, $\dot{\delta}_c/\dot{\delta}_s$. As noted in Fig. A-2, the two different approximations shift only the $\dot{\delta}_c/\dot{\delta}_s$ parameter along the curve a small amount, probably within the experimental accuracy of the known saturation rate and form of the saturation curve. Accordingly, it is recommended that the expressions for the simpler form of approximate gain given in Eq A-5 and A-21 be used for analytical purposes.

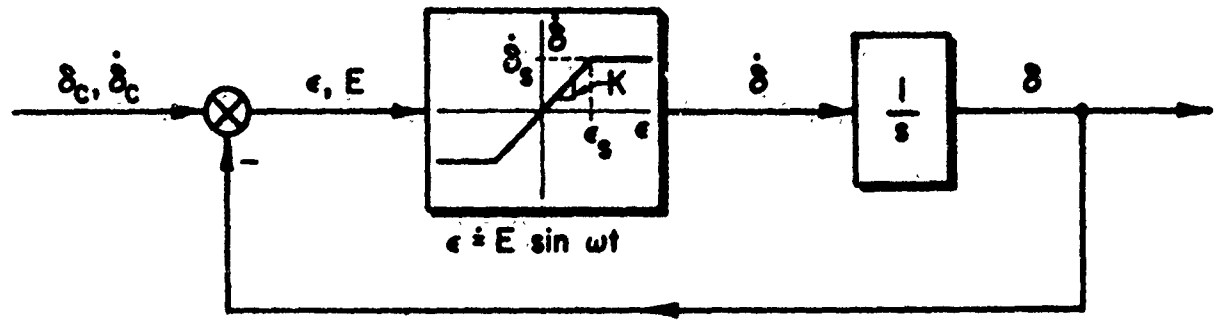

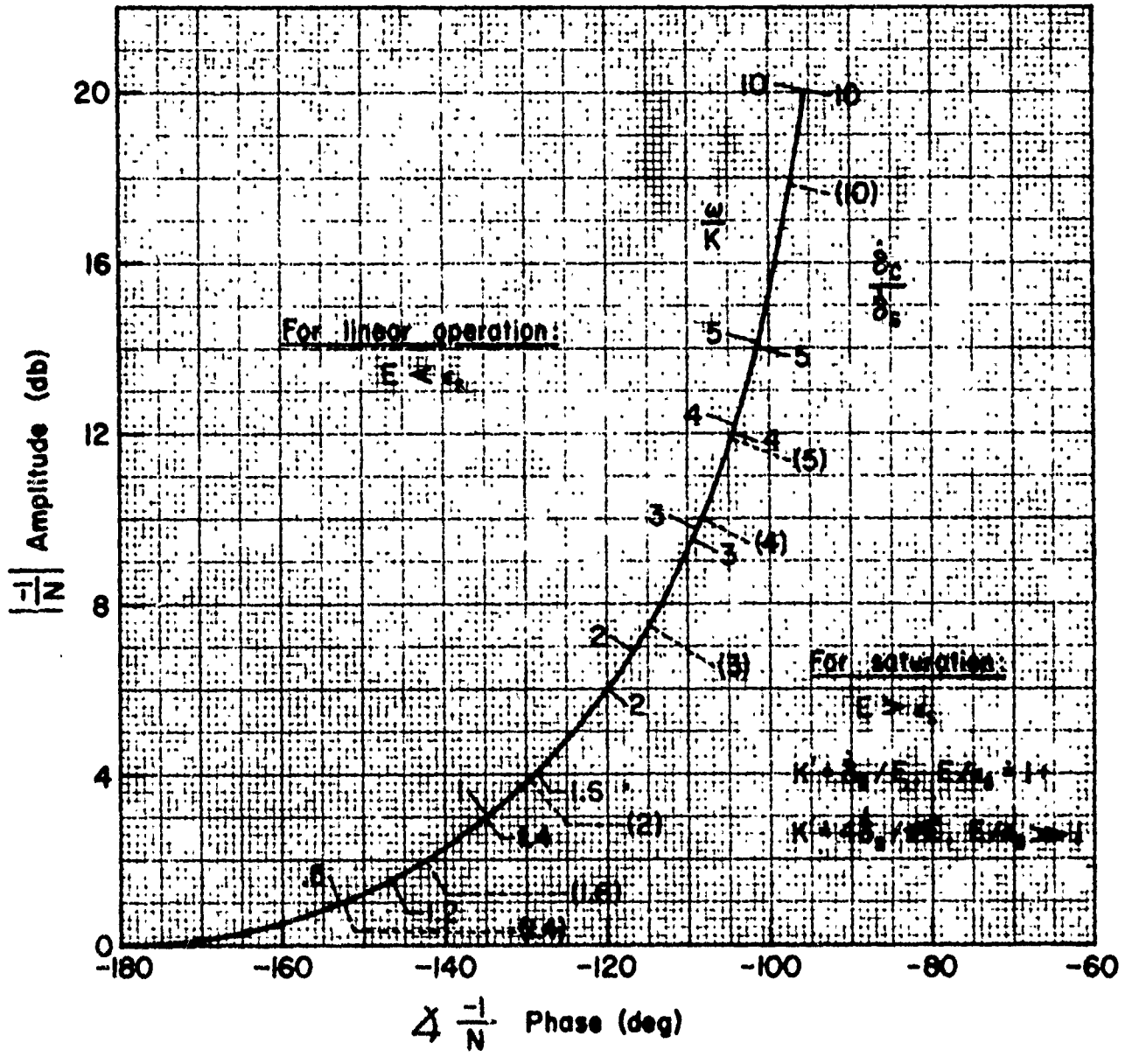

Figure A-2. The Negative Inverse Describing Function for a Rate-Limited Position Servo

CLASSIFIC

Examples shown as: SPECIES (Aircraft)

CLASS	I. [illegible]	
PITCH	IMPROPER SIMULATION[5]; D, V; a: Abnormally high value [illegible] and low [illegible] to [illegible] when regulating large disturbances. GCA-INDUCED PHUGOID (C-[illegible])[5]; I, V; b: [illegible] unstable closed-loop phugoid mode. ARM ON STICK (A4D-1)[7], (T-2A)[illegible]; F; a: Arm mass [illegible] feel [illegible] back to unstable coupling with short-period [illegible] pilot [illegible] onto stick after a large input.	PORPOISING (SB2C-1)[37]; F; [illegible] frequency speed and cl[illegible] J. C. MANEUVER (F-8[illegible]), ([illegible] large oscillations at [illegible] PITCH-UP (XF-104), (F-101B) [illegible] oscillations of varyi[illegible] maneuvers near the cri[illegible] LANDING PIO (X-15)[22]; S; [illegible] tion at short period.
LATERAL-DIRECTIONAL	ω_ϕ/ω_d EFFECT (X-15)[20], (T-33VSA)[21], (F-101B)[38], [illegible]; V; [illegible]: Zero of roll [illegible] closed-loop [illegible] at low [illegible] conditions. BORESIGHT OSCILLATIONS (F-[illegible]A); D, V; [illegible]: Spiral roll [illegible] degraded during gunnery.	
YAW	FUEL SLOSH SHAKING (KC-135A)[illegible], (T-[illegible]A)[illegible]; V; [illegible]: Fuel [illegible] with Dutch roll [illegible] when rudder used to stop yaw oscillation.	TRANSONIC SHAKING (A3D); [illegible] deflections, leading [illegible]
ROLL	NONE KNOWN	PILOT-INDUCED CHATTER (F-[illegible] attempted to control [illegible]

Legend:

Superscripts refer to references of occurrence.

Critical Subsystems:

D = Display
F = Feel system (except [illegible])
B = Bobweight
S = Power servo actuator
V = Vehicle (airframe)
A = Augmenter (damper)

[illegible] Flight Conditions:

- Low altitude, near-sonic Mach
- [illegible] approach or takeoff
- [illegible]

A

E. KNOWN PIO CASES

l Subsystem; Critical Flight Condition; Remarks

TYPE

ERIES NONLINEAR ELEMENTS	III. SUBSIDIARY FEEDBACK NONLINEAR ELEMENTS
s in stick versus elevator deflection resulted in low tone.	BOBWEIGHT BREAKOUT (X4D-1)[2,7], (T-38A)[1,4]; I, B; a: At high-g maneuvers the bobweight overcomes system friction and reduces apparent damping of the aircraft in response to force inputs, resulting in large oscillations at short period.
a: Valve friction plus compliant cabling resulted in	
6; V; c: Unstable kink in M(α) curve led to moderate-period (depending on extent and nature of the kink) during attack.	LOSS OF PITCH DAMPER
p around elevator rate-limiting caused moderate oscilla-	
	LOSS OF YAW DAMPER
eparation over rudder causes control reversal for small if rudder used to damp yaw oscillations.	
Small limit cycle due to damper aggravated whenever pilot	

B